Investigating the seasonal and interannual variability of the poleward undercurrent in the northern Benguela system

Sarah E. Yates

Department of Oceanography, University of Cape Town

November 2012

Abstract

The Benguela Current System is unique as both the equatorward and poleward boundaries are warm water current systems. Between 15 °S – 37 °S the surface currents are generally equatorwards, with 7 distinct upwelling cells, narrow equatorward shelf-edge jets and a poleward undercurrent along the continental slope. Model data was used to determine the seasonal and interannual variability of the poleward undercurrent (PUC) in the northern Benguela system. The PUC is the southward extension of the Angolan Current that carries low oxygen water (LOW) originating from the Angola Dome. The LOW flows from the Angolan region southwards in the Benguela system. The focus of the study is on the PUC associated with the Sverdrup relation. The model ORCA-025 was used to reproduce zonal transects from 17 °S to 30 °S to determine the changing characteristics of the PUC with latitude as well as seasonal and interannual variability of this current. The PUC is faster moving in the north (~17 °S) and decreases in velocity moving south (~30 S°). The PUC is shallower in the north increasing in depth in the south. The model data shows the velocity of the PUC has a seasonal cycle that is faster in the austral summer and autumn and weakens in the winter. The transport of the PUC is amplified during austral winter and spring, which is consistent with the increased negative wind stress curl during those seasons. The wind stress curl in the region exhibits a strong connection with the transport of the PUC via the Sverdrup relation. The PUC exhibits interannual variability when comparing to the Benguela Niño events, but does not show a correlation with El Niño Southern Oscillation.

Table of contents:

1. Introduction

The Benguela system is the eastern boundary system of the South Atlantic. The Benguela Current makes up the eastern limb of the South Atlantic Subtropical gyre (STG) (Veitch et al., 2006). It is one of the four upwelling systems in the world. It is also a unique system, as it is bounded by two warm currents namely the Angola Current at the northern boundary and the Agulhas Current to the south (Shillington et al., 2006; Veitch et al., 2006; Veitch et al., 2009). The Benguela upwelling regime extends to the southern tip of Africa from ~14 -16 °S. The northern boundary of the upwelling regime is the Angola Benguela Frontal Zone (ABFZ), the confluence of the Angola Current and the Benguela upwelling (Veitch et al., 2006) regime. The southeasterly wind associated with the South Atlantic Anticyclone (SAA) controls the upwelling of the Benguela system (Veitch et al., 2006). There are seven upwelling cells in the Benguela system, where the cell at Luderitz (~27.5 °S) separates the persistent upwelling in the north from the strongly seasonal upwelling in the south (Veitch et al., 2006). Low Oxygen Water (LOW) originating from the Angola Dome (north of ABFZ) in the tropical Atlantic is advected south into the northern Benguela upwelling regime, which often has catastrophic repercussions for living marine resources (Monteiro et al., 2006). The advection of LOW intensifies during late austral summer when the poleward undercurrent (PUC) strengthens (Veitch et al., 2006).

The PUC is defined as a persistent poleward flow of restricted width and thickness, which is bound to the continental slope and runs in the counter direction to the dominant regional circulation (i.e. Benguela Current) (Barton, 1989; Pizarro et al., 2002) and has been observed in other eastern boundary systems. The PUC in the northern Benguela has a width of less than 100 km with an average speed of ~10 cm.s^{-1} (at the level of strongest flow) (Barton, 1989) and an average transport of ~0.8 ± 0.2 Sv (Veitch et al., 2006). The PUC core is typically located at a depth of 200 to 300 m in the northern Benguela, which deepens moving south. There are two streams of PUC documented in the northern Benguela region (Penven et al., 2005). The one stream is associated with the upwelling regime, while the other stream is a curl-driven flow (Penven et al., 2005). The PUC shows seasonality with increased flow during the austral summer and early autumn that corresponds to the seasonal advection of LOW from the Angola Dome (Monteiro & van der Plas, 2006). The PUC stream associated with the Sverdrup relation (curl-driven flow) will be the focal point of this study.

The focus of this study is to examine the seasonal and interannual variability of the PUC associated with the Sverdrup relation in the northern Benguela system. There has been limited research done on the PUC in this region. The kinematics of the PUC has not been explored, such as the cross-flow processes, in order to understand the along-shore continuity and the sources and sinks of the PUC (Mooers, 1989; Pierce et al., 2000). There has been limited research on this current as it is difficult to obtain long-term time series of current measurements along-shore and how the vertical and horizontal structure of the PUC responds to forcing (Mooers, 1989). Regarding all the eastern boundary currents there has been limited research done on seasonal and interannual variability of the PUC and how the variability relates to the wind (Barton, 1989; Pizarro et al., 2002).

There have been several studies that have measured the PUC using current and biogeochemical measurements (Monteiro et al., 2006). The aim of the project is to use a model product namely ORCA-025, to investigate the PUC in the northern Benguela. The use of the modeling tools will also lead to understanding the seasonal and interannual variability of this current. The investigation of the PUC may lead to improved knowledge on the impacts on the ecosystem from transport of LOW. The impacts of LOW have a close link with elevated sulphide concentrations, which results in significant losses of demersal and bottom species. LOW has been identified as a key factor that governs the variability and commercial viability of the fisheries in the region (Monteiro & van der Plas, 2006). By exploring the variability of the PUC it can improve the forecasting capabilities of LOW transport, which could assist with ecosystem management and sustain fisheries management. Since the Benguela current confluences with the warm Angola Current and has the phenomena of Benguela Niños, it is a unique area to observe the influence of the PUC in this region.

In order to address the seasonal and interannual variability of the PUC in the northern Benguela region, the following questions have been considered:

- What are the poleward undercurrent characteristics and how do they change with latitude?
- What is the seasonality of the poleward undercurrent?
- What is the interannual variability of the poleward undercurrent?
- What are the atmospheric drivers of the poleward undercurrent?

The structure of the study starts with an overview of the Benguela System and the importance of salient features in the northern region. The significance of the PUC is outlined followed by the model data and methods used to investigate the variability of the current. A description of the domain is provided to present a setting for the environment of the region. The findings of the characteristics, variability and atmospheric controls of the PUC are shown to understand the seasonal and interannual cycles of the current. Further discussion is provided highlighting the variability and how it connects with atmospheric controls. Lastly, in concluding remarks, a summary to each key question.

2. Literature Review

2.1 Overview of the Benguela Current System

The Benguela Current is one of the four eastern boundary currents and is situated off the west coast of Africa, 5-37 °S, 0-26 °E (Shillington et al., 2006; Veitch et al., 2006). It is a unique current because warm water currents bound it on the equatorial and poleward extremities (Shillington et al., 2006; Veitch et al., 2009). The warm water currents are the Angola Current in the tropical Atlantic Ocean and the Agulhas Current in the Indian Ocean (Veitch et al., 2009). The Benguela current makes up the eastern limb of the Subtropical Gyre (STG) and consists of cool nearshore water, which is the Benguela upwelling regime (Veitch et al., 2006). Generally, the surface currents are equatorwards between 15 °S and 37 °S with coastal upwelling cells, a narrow equatorward shelf-edge jets and a PUC along the continental slope (Shillington et al., 2006). The Benguela upwelling system is divided into a northern and southern regime by large-scale and nearshore dynamics that interact differently with topography (Veitch et al., 2009) (refer to Figure 2.1 to view the geographic location.) The upwelling cell at Luderitz (at 27 °S) is the divider of the northern and southern Benguela (Hutchings et al., 2009; Veitch et al., 2009). There are 7 distinct upwelling cells in the Benguela system. The three southern cells have a strong seasonal signal with the greatest upwelling in spring and summer. The two northern cells have less of a seasonal signal and the central cell (Luderitz, 27 °S) has year-round upwelling (Veitch et al., 2006). The disparate seasonal cycle of the northern and southern Benguela upwelling regions is a result of differences in the meridional wind regime (Veitch et al., 2009). The dominant physical forcing mechanism of the Benguela upwelling region is the South Atlantic Anticyclone (SAA) (Giraudeau et al., 2000). The seasonal shifts of the high-pressure system are responsible for the temporal variability of the upwelling-favorable winds (Giraudeau et al., 2000).

2.2 Large-scale flow regime

The Benguela current lies offshore of the upwelling region and makes up the eastern limb of the South Atlantic STG (Veitch et al., 2009). The water masses of the Benguela current is supplied by the southern limb of the STG, as well as south Indian Ocean waters via the Agulhas current (Veitch et al., 2009). The northern margin of the Benguela upwelling area is the Angola Benguela Frontal Zone (ABFZ), which is the confluence of the warm Angola current and the cool upwelling regime (Shannon et al., 1987; Veitch et al., 2009). Figure 2.1 highlights the salient features of the Benguela system.

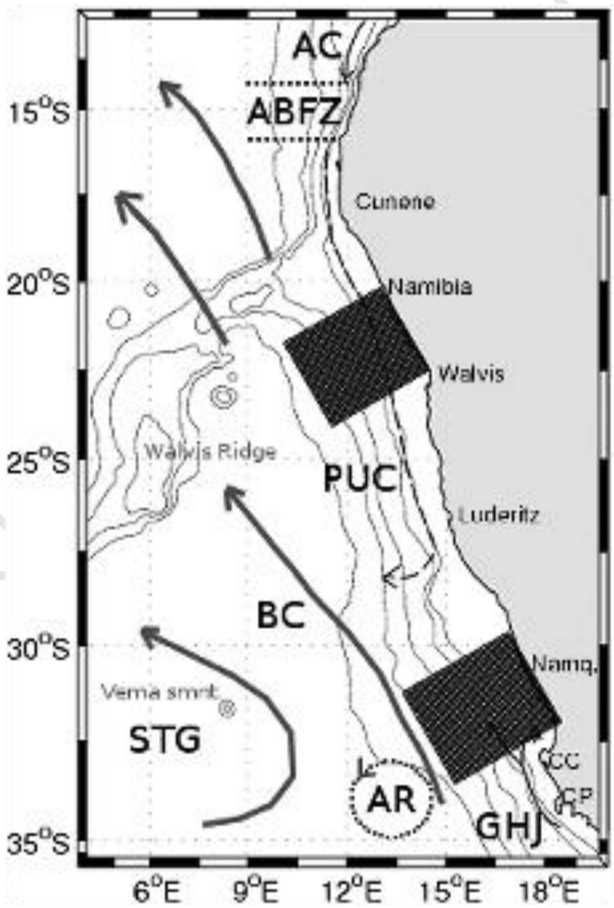

Figure 2.1: The figure shows the large scale and mesoscale features in the Benguela System. Namely, the Benguela Current (BC), Agulhas Rings (AR), GoodHope Jet (GHJ), Subtropical Gyre (STG), Poleward Undercurrent (PUC), Angola Benguela Frontal Zone (ABFZ) and Angola Current (AC). (Veitch et al., 2010).

The Angola Current is influenced by the input from the South Equatorial Current (SEC) and the South Equatorial Counter Current (SECC) at 5 °S (Shillington et al., 2006). This region is fed with water from the Equatorial Under Current (EUC), the Gabon Current (GC), the South Equatorial Counter Current (SECC) and the South Equatorial Under Current (SEUC) (Rouault et al., 2007), as shown in figure 2.2.

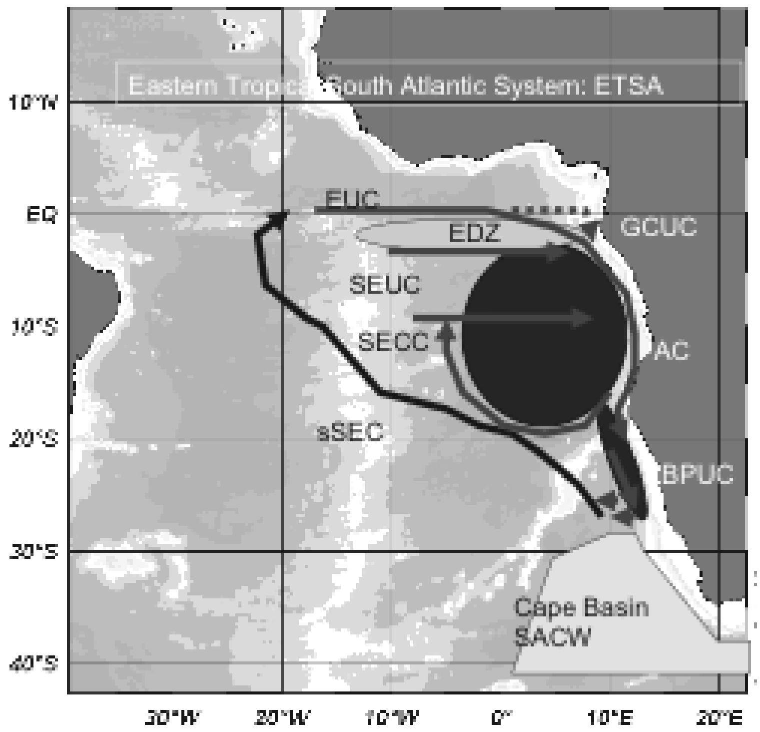

Figure 2.2: The Eastern Tropical South Atlantic System shows the Equatorial Under Current (EUC), Equatorial Divergence Zone (EDZ), Guinea-Congo Under Current (GCUC), South Equatorial Under Current (SEUC), South Equatorial Counter Current (SECC), Angola Current (AC), South Equatorial Current (sSEC), Benguela Poleward Under Current (BPUC), and South Atlantic Central Water (SACW) Cape Basin. (Monteiro & van der Plas, 2006).

2.3 Upwelling regime

The atmospheric forcing for the Benguela upwelling regime is the semi-permanent SAA, producing southerly wind stress near the west coast (Hardman-Mountford et al., 2003; Shillington et al., 2006; Veitch et al., 2009). The upwelling is controlled by the SAA and the seasonal shift of the SAA results in seasonal variations of the upwelling along the southwest coast (Veitch et al., 2006). In the austral summer, a low-pressure system develops over the continent, which enhances the zonal pressure gradient, leading to an intensification of the southerly wind stress (Shillington et al., 2006). In the austral winter, the main atmospheric circulation features shift north so that the majority of the Benguela region is subject to low level southerlies (Shillington et al., 2006). The shift of the SAA results in variation of the upwelling-favorable winds; when the SAA is in its northernmost position there is little upwelling in the southern Benguela region during the winter (June-August). When the SAA is in its southernmost position, upwelling is enhanced in the southern Benguela region during the summer. In the northern Benguela region, upwelling is mostly perennial but more pronounced in the winter and early spring (April-November) (Giraudeau et al., 2000). Between 15 °S and 30 °S there is year-round upwelling, with seasonal upwelling between 30 °S and 34 °S (Shillington et al., 2006).

The coastal upwelling regime of the Benguela system is characterized by cyclonic (negative) wind stress curl near the continental boundaries and anitcyclonic wind stress curl 200km offshore (Bakun & Nelson, 1991). The negative wind stress curl along the southwest African coast is shown in figure 2.3. Towards the coast, there is a decay of wind stress, which defines the region of cyclonic wind stress curl (Bakun & Nelson, 1991). Ekman pumping occurs where there is coastal upwelling that is enhanced by curl-induced oceanic upwelling (Bakun & Nelson, 1991; Risien & Chelton, 2008). The alongshore wind stress drives the upwelling system. Figure 2.4 represents the transport of the large-scale flow regime of the Benguela in the upper 1000 m, which shows the division of the regime (Veitch et al., 2010) and the streamfunction derived from the Sverdrup relation from 0.5° QuikSCAT wind product and integrated from the west coast of southern Africa (Veitch et al., 2010). The negative wind stress curl has the potential to enhance it and is the principle for the development of the PUC (Veitch et al., 2010). The PUC is strongly seasonal as is the wind stress curl; the poleward flow in the northern Benguela intensity increases when the wind stress curl is most negative (Veitch et al., 2010). The poleward flow exists due to the wind stress curl in agreement with the Sverdrup relation; the southward flow below a shallow surface layer is directly forced by the wind stress curl in the Peru-Chile Poleward Undercurrent (Penven et al., 2005), the Peru-Chile Poleward Undercurrent exists at different latitudes, thus the exploration of the Benguela PUC in relation to wind stress curl.

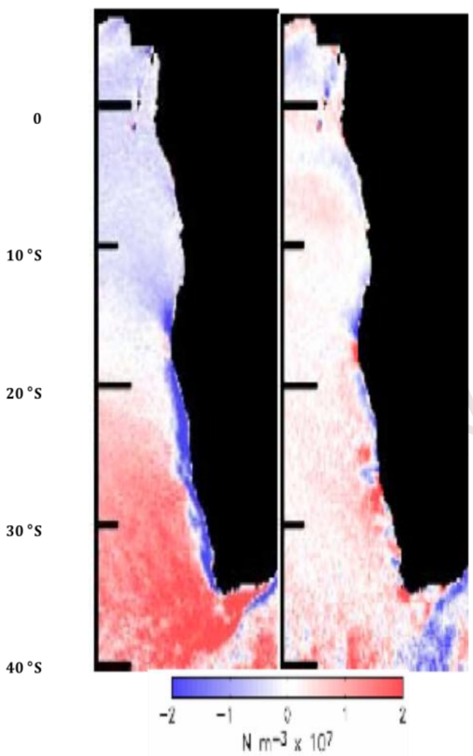

Figure 2.3: Four-year average wind stress curl (left) and divergence (right). Image shows negative wind stress curl along the southwest African coast. (Shillington et al., 2006)

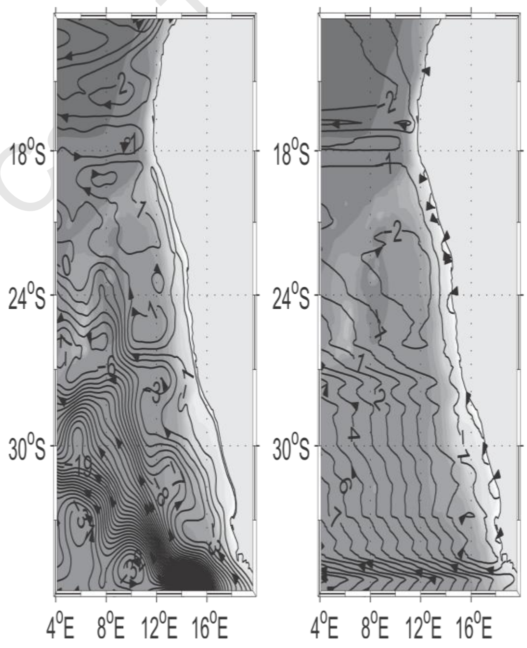

Figure 2.4: Annual mean transport streamfunction integrated from 0-1000 m depth (left). The Sverdrup streamfunction with contour interval= 1 Sv (right). Shades of grey represent bathymetry. (Veitch et al., 2010).

2.4 Water masses

The water mass structure in the Benguela system consists of tropical water entering from the Angola Basin and northern Benguela. The Benguela Current is composed of a mix of Indian and South Atlantic subtropical thermocline water, with low oxygen tropical Atlantic water and cooler subantarctic water (Hardman-Mountford et al., 2003). Antarctic Intermediate Water (AAIW) forms at the surface of sub-polar and polar regions and is characterized by a high salinity minimum deep in the water column in the northern and southern Benguela, the AAIW water mass sits at a depth of 750 – 800 m. Water from the Angola Basin with high AAIW salinity signal enters the northern Benguela in a PUC along the shelf-edge (Shillington et al., 2006). The South Atlantic Central Water (SACW) in the Benguela has a relatively high salinity originating in the tropical Angola Basin (Shillington et al., 2006). The central and intermediate water masses come from the oxygen-depleted Angola Basin (Duncombe Rae, 2005) in the northern Benguela. The vertical sections across the shelf shows high salinities constrained to the shelf-edge, which is consistent with a PUC of Angola Basin origin (Shillington et al., 2006). This has implications on the dispersion of Low Oxygen Water (LOW) and triggers anoxic events along the shelf (Duncombe Rae, 2005). LOW is transported in the SACW at a depth of 200 – 400 m (Mohrholz et al., 2008). The anoxic conditions can have decimating effects of marine resources resulting in increased mortality, decreased abundance and availability of commercially fished stocks (Monteiro et al., 2006).

2.5 The Angola-Benguela Frontal Zone (ABFZ)

The Angola Current is a southward moving surface current that converges with the cool Benguela upwelling regime at the Angola Benguela Frontal Zone (ABFZ) at 15-17 °S (Hardman-Mountford et al., 2003; Shillington et al., 2006; Veitch et al., 2006). The Angola Benguela Front (ABF) has a strong thermal gradient with seasonal and interannual changes in its location (John et al., 2004; Veitch et al., 2006; Hutchings et al., 2009). The width of the ABFZ fluctuates seasonally; in the austral winter it exists between 16-17 °S and in the austral summer it exists between 15.5-17 °S. As well as being broader in the summer the ABFZ extends further offshore in the spring and summer (Veitch et al., 2006). The ABF is well defined in the austral summer, when it shifts to its most southern position, while in the winter the front is less defined and positioned farther north (Colberg & Reason, 2006; Colberg & Reason, 2007). There is a net annual modeled transport of 0.45 Sv near the surface tropical water flowing across the ABF (Rouault et al., 2007; Rouault, 2012). El Niño Southern Oscillation (ENSO) and wind stress curl (Colberg & Reason, 2007) induces the ABFZ variability. The strength of the frontal zone is related to the strength of the southerly wind stress that controls the coastal upwelling (Colberg & Reason, 2007). ENSO is anticipated in the South Atlantic region by means of the Pacific South American wave train that induces changes in strength and position of the South Atlantic Anticyclone (Colberg & Reason, 2007).

2.6 Benguela Niños

Benguela Niños have similarities to the warming in the South American El Niño (Rouault, 2012). During a Benguela Niño, there is an intrusion of equatorial warm water moving southward along the coast of northern and central Namibia (Shannon et al., 1986; Gammelsrϕd et al., 1998). There are several warm and cool periods in the Benguela region off the southwestern coast of Africa (Shannon et al., 1986). Benguela Niño is less pronounced and less frequent than the Pacific El Niño and the effect of these events is limited to the northern Benguela region (Shannon et al., 1986). Major Benguela Niño events occurred in 1963, 1984, 1995 and 2001 with major cold events in 1983, 1991/1992 and 1996/1997 (Rouault, 2012). Benguela Niños are triggered by the relaxation of the equatorial winds in the western Atlantic (Rouault, 2012); this generates free equatorial Kelvin wave propagation along the equatorial wave-guide, which continues along the west coast (Fennel, 1999; Lass et al., 2000; Pizzaro et al., 2002). Kelvin waves may be a possible reason for the occurrence of the poleward flow south of the ABF (Fennel, 1999). This warm advection is an important role in the development of Benguela Niños (Rouault, 2012). The Benguela Niños peak in late austral summer and last for several months (Rouault, 2012); however, the seasonal signal in the Atlantic is stronger than the interannual signal (Shannon et al., 1986).

2.7 Poleward Undercurrent (PUC)

All eastern boundary currents have a PUC (Mooers, 1989; Nelson, 1989). A PUC may be defined as a persistent, poleward flow that has restricted width, which is bound to the continental slope. It runs in the direction counter to the dominant regional circulation and may at particular times and positions extend upwards to the sea surface (Barton, 1989; Fennel et al., 2012). At the eastern boundary, undercurrents generally have a core speed of ~0.1m.s^{-1} and a mean volume transport of 0.8 ± 0.2 Sv (Mooers, 1989; Pierce et al., 2000). A shelf-edge poleward flow exists in the northern Benguela region, which is primarily driven by wind stress curl via the Sverdrup relation (McCreary et al., 1985; Skogen, 1999; Veitch et al., 2006). A crucial role is played by the wind stress curl, which structures the oceanic reaction through Ekman pumping (Fennel et al., 2012). It is strongly seasonal, with the highest intensities in the spring and summer when the wind stress curl is most negative (Veitch et al., 2006). When there is the presence of downward sloping isopycnals below 200m towards the coast, it is indicative of a geostrophic southward flow at that level (McCreary et al., 1985; Barton, 1989; von Bodungen et al., 2008). Figure 2.5 illustrates how the Regional Ocean Modeling System (ROMS) shows the PUC by the downward sloping isohalines. The sloping isohalines at the shelf edge indicate the presence of the PUC between 200 and 600 m. The presence of the shelf weakens the PUC (McCreary et al., 1985). The northern Benguela southward flow is observed to have transport of 1 Sv and is an important link between the cyclonic gyre in the Angola Dome area and the source region for the Benguela Current (Lass et al., 2000). The PUC crosses the ABFZ along the shelf-edge, where it is near the surface north of the front and at the upper slope depth (250-500 m) south of the front (von Bodungen et al., 2008). Observations in the northern Benguela region show that oxygen depleted, with nutrient-rich SACW water between 200m and 700m is advected polewards, at least to 22 °S (von Bodungen et al., 2008), along the coast from the area of the Angola Dome; which is a pool of oxygen depleted water (Lass et al., 2000). This transport of low oxygen and high nutrient into the Namibian shelf can lead to adverse effects on commercial resources, such as the fisheries (von Bodungen et al., 2008). The PUC is characterized by 9 °C, 34.7 salinity at ~400m (shelf-break) and between 6-8 °C, 34.48-34.68 salinity at 350m-500m (near shelf-break) (Dingle & Nelson, 1993).

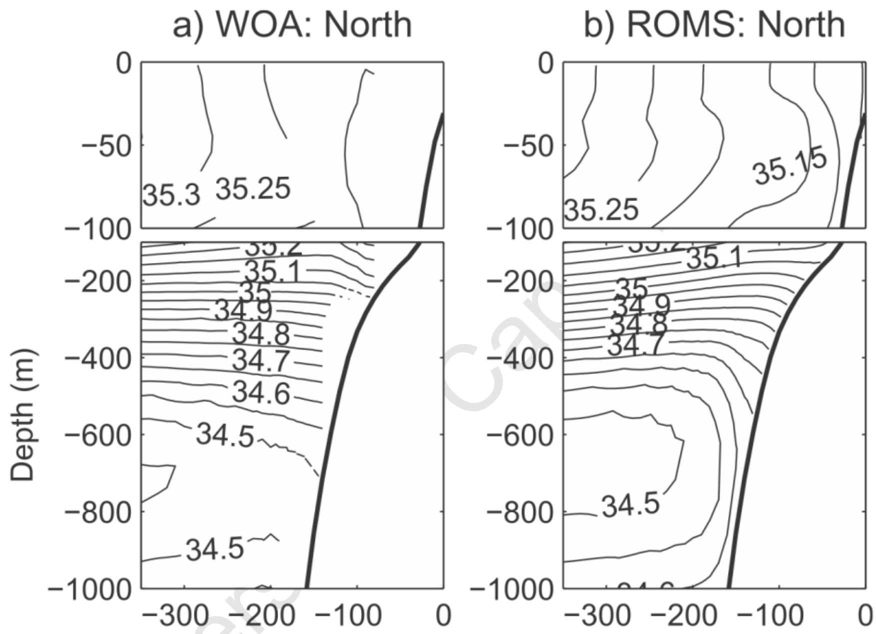

Figure 2.5: Alongshore average salinities comparison between measured data and the model ROMS. Downward sloping isohalines in b) show the presence of the PUC in the northern Benguela region (Veitch et al., 2010).

According to Clarke (1989), the two main mechanisms that drive the near-shore small-scale PUC are the mean flow generated by oscillatory flow over small amplitude; small scale bumps in the shelf topography and coastal-trapped waves always propagate polewards, so the oscillatory current is flowing equatorwards. According to Nelson (1989), the large-scale PUC in the Benguela region is driven by the Sverdrup theory (wind stress curl) and is modulated by Kelvin waves from the equator and upwelling dynamics. According to Penven (2005), the Peru-Chile PUC has two distinct cores of poleward flow, where the one corresponds to the coastal upwelling-driven undercurrent and the other corresponds to curl-driven flow.

2.7.1 Sverdrup theory

The wind stress curl drives a mean poleward flow, which is in agreement with Sverdrup dynamics (Penven et al., 2005).

Sverdrup relation:

$$\beta V = \frac{\nabla \times \tau_s}{\rho_0}$$

V is the $\frac{\delta\psi}{\delta x}$ change in streamfunction over the change in x, β is the rate of change of Coriolis parameter with latitude, ρ_0 is the reference density of seawater (1025 kg.m^{-3}), and τ [N.m^{-2}] is the wind stress (Penven et al., 2005). (For derivation of the Sverdrup equation refer to Appendix.) The wind stress curl (via the Sverdrup theory) has been shown to be the driving force of the poleward flow, which is the strongest during spring and summer when the wind stress curl is most negative (Penven et al., 2005; Veitch et al., 2010). During the summer the peak poleward transport is farther offshore, when the cyclonic wind stress curl has greater intensity (Veitch et al., 2005). The wind stress curl via the Sverdrup relation causes the poleward flow in the northern Benguela and its offshore advection at 27 °S. The offshore veering is related to the wind stress curl interacting with the northwestward path of the Benguela Current (Veitch et al., 2010). The Sverdrup relation does not hold for the southern Benguela due to the inflow of the Agulhas Current and eddy fluxes associated with the Agulhas Current (Veitch et al., 2010).

2.7.2 PUC associated with coastal upwelling

Like all the poleward undercurrents in eastern boundary systems, the Benguela PUC may be modulated by upwelling favorable alongshore winds (Pizarro et al., 2002). Coastal upwelling is a phenomenon linked with the generation of Kelvin waves and these waves control the development of the PUC over the shelf (Suginohara, 1982). The shelf-edge upwelling is maintained by the wind stress curl fluctuations with time scales of less than a few months since it is restricted by propagating long baroclinic Rossby waves (Lass & Mohrholz, 2008). In an idealized model study, the arrival of barotropic Kelvin waves along the coast start to accelerate a coastal undercurrent in the opposite direction to the wind (Philander & Yoon, 1982). Kelvin waves alter the vertical structure of the coastal current so that the subsurface undercurrent layer is accelerated (Philander & Yoon, 1982). Hart & Currie (1960) proposed that a PUC along a shelf-edge would compensate for water removed from 200-300m level by perennial upwelling. The PUC is thus a 'compensation current', which provides replacement source for water that is upwelled (Mooers, 1989; Smith, 1989). Where there is seasonal change in Ekman transport (upwelling), there will consequently be a seasonal change in the poleward compensation current or PUC (Mooers, 1989; Nelson, 1989).

2.7.3 The role of the PUC in transporting Low Oxygen Water (LOW)

The Angola current is important for the study as it intrudes into the northern Namibian waters, carrying tropical fish larvae (John et al., 2002). The Angola current splits into to two streams; the main flow closes the Angola gyre while its extension becomes the Benguela PUC along the Namibian shelf to 27 °S (Monteiro & van der Plas, 2006). The oceanic low oxygen water (LOW) reservoir was generated by productivity in the Angola Dome area (Monteiro & van der Plas, 2006). The advection link between the low oxygen pool in the Angola Dome and the northern Benguela is important as there is LOW variability coupled to upwelling that peaks in June to August (Monteiro & van der Plas, 2006). During the austral summer it is apparent that anoxic bottom waters are present at the central Namibian shelf, transported by the PUC from the Angola Dome (Mohrholz et al., 2008). The strength of the PUC determines the occurrence of anoxic waters in the northern Benguela region (Mohrholz et al., 2008). The occurrence of LOW has the ability to lead to harmful algal blooms in the northern Benguela region, having an adverse effect on the fisheries (Monteiro et al., 2006).

2.7.4 Seasonal and interannual variability

The PUC is strong in the austral summer (Lass & Mohrholz, 2008), but weakens in the winter as the meridional flow is largely northwards (Mohrholz et al., 2008). The PUC associated with upwelling dynamics tends to show seasonal and interannual variability, however, the PUC related to the Sverdrup relation has shown seasonal variability but the interannual variability has not been thoroughly explored. The mid-latitude El Niño response of poleward undercurrents may be connected to the poleward propagating disturbances (Mooers, 1989). The wind stress curl in the Benguela region has a local effect on the PUC, whereas Benguela Niños and ENSO have a remote effect. The Benguela Niños events transpire at an interannual variability scale of the northern Benguela region, occurring less frequently than ENSO events. The Benguela Niños have a more direct effect in the Atlantic than ENSO (Shannon et al., 1986). Pizarro et al. (2002) states that the seasonal variability of the PUC, when associated to coastal upwelling, is related to equatorial variability. This variability is modulated at seasonal and interannual periods by Rossby waves forced by equatorial Kelvin waves approaching the coast (Pizarro et al., 2002). It is possible that the poleward undercurrents influence local annual cycles of biological production, since the undercurrent provides upwelling source water along the coast (Pizarro et al., 2002).

3. Data and Methods

3.1 ORCA-025 configuration

In order to investigate the seasonal and interannual variability of the poleward undercurrent in the northern Benguela System, ocean model OPA with ORCA-025 configuration was used (Timmerman et al., 2005). ORCA-025 is a reanalysis model using model outputs and *in situ* data.

The ORCA-025 configuration is designed to capture the prominent features of the tropical Atlantic. ORCA-025 is a primitive equation, z-coordinate, global eddy permitting ocean/sea-ice model, developed for the DRAKKAR project (Barnier et al., 2006). It has a horizontal grid resolution of ¼ degree at the equator, leading to the horizontal dimensions 1442 x 1021 grid points (Barnier et al., 2006). In the vertical grid there are 46 levels, with grid spacing from 6 m near the surface to 250 m spacing at 5750 m (Molines et al., 2006; Barnier et al., 2006). ORCA-025 has duration of 47 years from 1958 to 2004. The maximum depth of the model is 5844 m; the deepest cell having a thickness of 500 m in deep basins. The effective resolution gets finer with increasing latitudes and is ~27.75 km at the equator, ~13.8 km at 60 °S or 60 °N (Barnier et al., 2006).

The initial conditions of the model for temperature and salinity were derived from Levitus 98 data set for the mean and low latitudes (Molines et al., 2006). All runs are performed with free surface, constant volume formulation (Molines et al., 2006). The forcing of the model is 6-hourly ERA-40 winds (1958-2001) at 10 m scalar wind field and ECMWF analysis winds (2002-2004), with a surface momentum flux that is directly provided as a wind stress vector (Barnier et al., 2006).

3.1.1 Hydrographic sections

To obtain a better understanding of the dynamic flow of the poleward undercurrent, five transects were extracted at 17 °S, 20 °S, 24 °S, 27 °S and 30 °S, as shown in figure 3.1. Two sections were extracted to examine the poleward undercurrent in the northern Benguela. The section in the northern-most region for transects T1, T2 and T3 was extracted, extended from 10 °S to 30 °S and 6 °E to 14 °E. The second section in the southern-most region for transects T4 and T5 was extracted, extended from 10 °S to 30 °S and 9 °E to 16 °E, each domain contained 24 vertical levels. Only 24 levels were used to capture the top 1000m where the PUC is located. The northern-most domain was chosen to include more ocean and less land, as the land juts out further west than the land in the southern domain. The time period that was focused on was from 1979 to 2004, because of improved accuracy in more recent years and it provides sufficient time to view any interannual variability. The transects were used to look at the different aspects, namely, velocity, salinity, seasonal and monthly velocities. The transport, anomalies and Nino 3.4 correlation were deduced from the monthly average velocities at each transect.

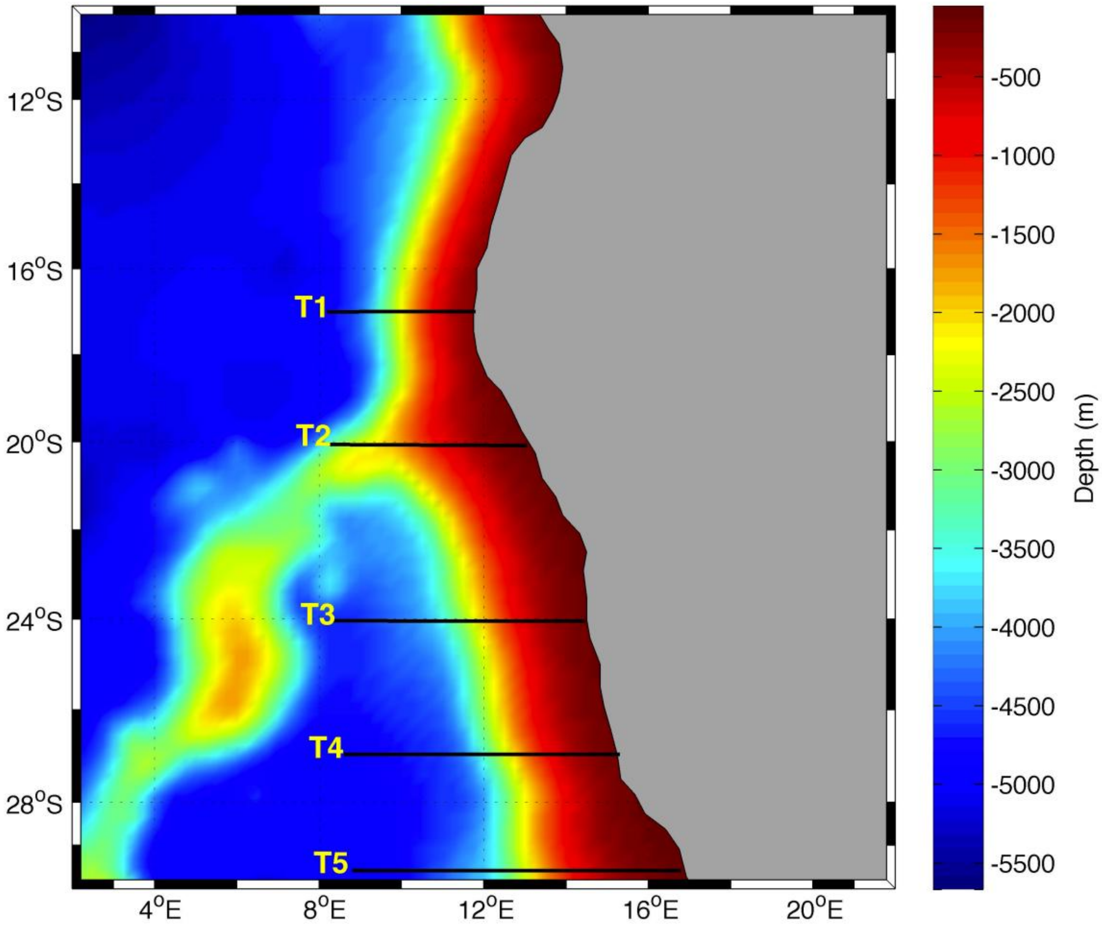

Figure 3.1: shows the location of the 5 transects used to explore the regime of the poleward undercurrent. T1=17 °S, T2=20 °S, T3=24 °S, T4=27 °S, T5= 30 °S.

3.2 Nino 3. 4 correlation

To examine the interannual variability of the poleward undercurrent, a correlation with Nino 3.4 (http://climexp.knmi.nl) was made. A correlation was made using the Pearson linear correlation coefficient between the two variables (correlation coefficient matrix). It measures the strength of the linear dependence between the two variables. The raw data of monthly climate indices Nino 3.4 was downloaded from Climate Explorer to correlate with the anomalies derived from the transect velocities.

Nino 3.4 index consists of sea surface temperature (SST) anomalies in 5 °S to 5 °N, 120 °W to 170 °W. From 1950 to present the data is from CPC (Reynolds OI SST) (http://climexp.knmi.nl). To correlate with the anomalies, Nino 3.4 index was taken from years 1979 to 2004.

3.3 Optimum Interpolated Sea Surface Temperature

The Optimum Interpolated Sea Surface Temperature (OI SST) data set was used to validate the model. This satellite SST data set is from National Oceanic and Atmospheric Administration (NOAA). OI SST has a resolution of 1 degree, which is compared to the ¼ of a degree resolution of ORCA-025. The OI SST data consists of satellite data monthly means from 1982 to 2004 (www.esrl.noaa.gov).

3.4 World Ocean Atlas (WOA)

World Ocean Atlas (WOA) 2005 salinity data was used to compare to ORCA-025 annual mean salinity. WOA05 is a set of objectively analyzed (1 degree grid) climatological fields of *in situ* salinity at standard depth levels for annual, seasonal, and monthly compositing periods for the ocean (http://www.nodc.noaa.gov).

3.5 Calculation of wind stress curl

ERA-40 6-hourly winds from years 1958 to 2002 were used to calculate the wind stress curl. Years 1979 to 2002 were used to calculate wind stress curl, to correspond with similar years of transport (1979 to 2004). The zonal and meridional velocities of the wind in each domain were used to calculate wind stress. The neutral wind stress was computed following Large and Pond (1981), where the neutral wind stress is given the wind speed at height z and air density is assumed to be constant at 1.2

kg/m^3. From the zonal (Z_x) and meridional (Z_y) wind stress the wind stress curl was calculated using the following equation:

$$\frac{1}{\rho_0}\left[\frac{\partial}{\partial x}\left(\frac{\tau^y}{f}\right)-\frac{\partial}{\partial y}\left(\frac{\tau^x}{f}\right)\right]$$

4. Results

4.1 Model Data

4.1.1 Evaluation of model

The validation of the model was done by comparing the SST of ORCA-025 at ¼ of a degree resolution to NOAA OI SST at 1-degree resolution. The OI SST data has a coarser resolution, but it highlights the main features of the Benguela system (figure 4.1). The satellite data shows the upwelling region and the ABFZ at ~ 16 °S. The model manages to highlight the upwelling region and the ABFZ, however, the model is ~ 1-2 °C warmer to that of the *in situ* data. Although the general pattern of the model agrees with the satellite data, there are different degrees of magnitude that exist. Figure 4.1 shows the greatest difference between 14 -18 °S and 21 – 25 °S along the Namibian coastline, due to the coarser resolution of the satellite data. Figure 4.1 shows the annual mean difference in SST between the model and observed data.

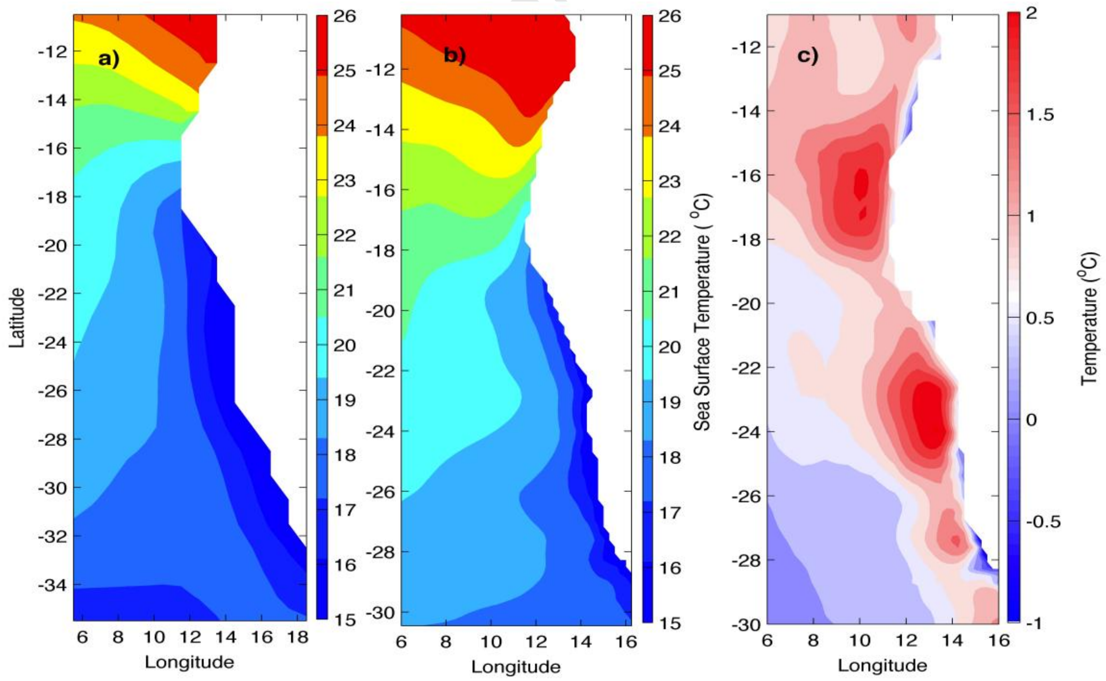

Figure 4.1: annual means of a) OI SST at 1 degree resolution for the Benguela region. b) ORCA-025 SST at ¼ degree resolution for the Benguela region c) annual mean OI SST-ORCA SST difference.

The model tends to show a warm bias (red) along the coast of ~1-2 °C. The cold biases (blue) are inshore (at 14 °S, 21 °S, 26 °S and 29 °S) and further offshore (in the south-west corner of the domain). With the finer resolution (1/4°) of the model a reasonable representation of the Benguela system is provided. Figure 4.2 represents the monthly SST climatologies for ORCA-025 and OI SST at the ABFZ (14.5 – 17.5 °S, 8.5 – 11.5 °E). This shows that in ORCA-025 the annual minimum and maximums are a month earlier than indicated by OI SST. The seasonal mean SST over the period 1982 to 2004 (Figure 4.3) at the ABFZ (14.5 – 17.5 °S, 8.5 – 11.5 °E) shows that ORCA-025 follows the seasonal trend well and captures the higher temperatures observed in 1984, 1995 and 2001, which are years of the Benguela Niño, but underestimates temperature minimums consistently. In winter ORCA-025 is warmer (~1-2 °C) than it should be.

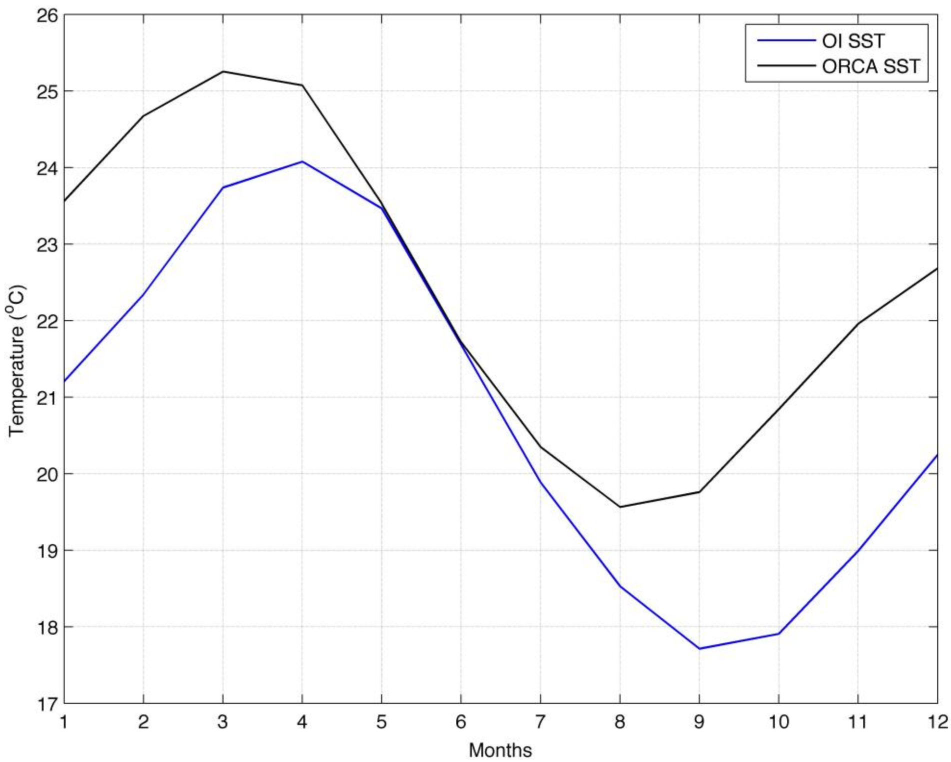

Figure 4.2: monthly SST climatologies for ORCA-025 and OI SST at the ABFZ.

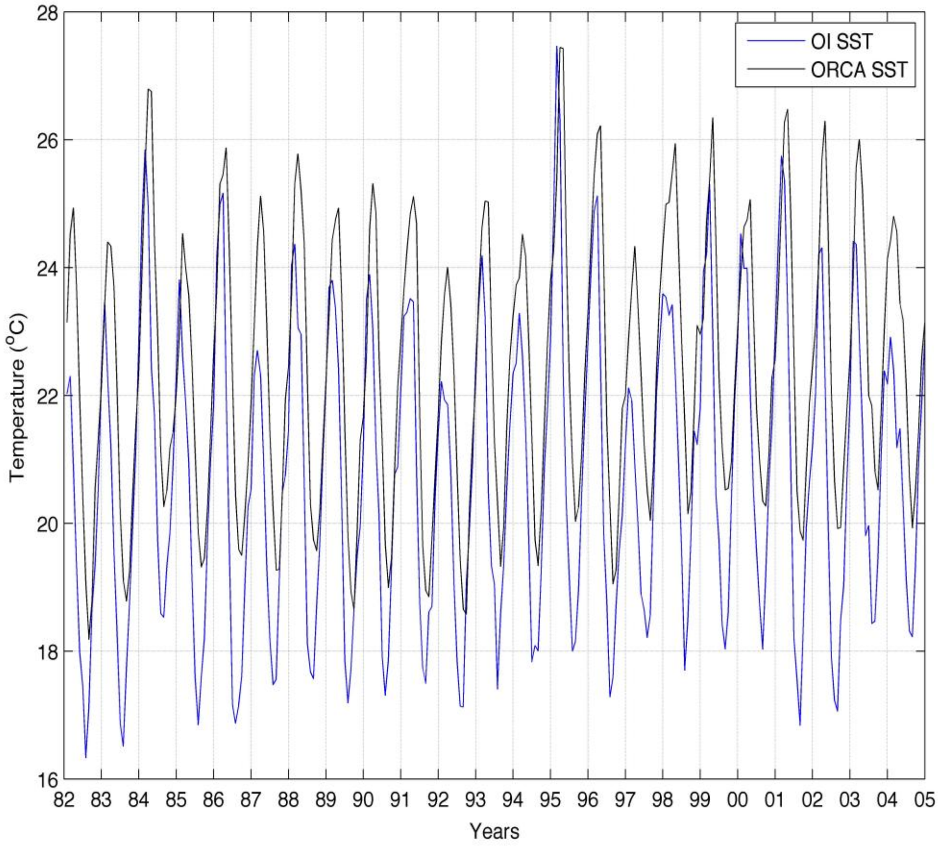

Figure 4.3: seasonal means of SST over the period 1982 – 2004 at the ABFZ.

Figures 4.4, 4.5 and 4.6 show annual mean salinity section comparisons between ORCA and equivalent climatological mean of WOA05. Figure 4.4 is at 17 °S shows the model agrees well with the *in situ* data, however, the PUC is not indicated as a shallow current (~ 100- 300 m) at this latitude, but shows a hint of a current at ~ 750 m in the WOA transect. At 17 °S and 24 °S the model shows downward sloping isohalines, which is an indication of the PUC. The downward sloping isohalines at a depth range of 100 m to 650 m suggest the presence of the poleward undercurrent. The WOA05 dataset section at 24 °S does not resolve for ~100km coastal band, however, there is a hint of downward sloping isohalines suggest the presence of the PUC at ~300 – 650 m. At 30 °S (figure 4.6) the model suggests there is a PUC at depths ~350 - 600 m and the *in situ* data does not suggest the presence of a PUC. At 30 °S, the isohalines in WOA transect do not show a downward slope, as the current has become much deeper and weaker or has dissipated in the southern Benguela.

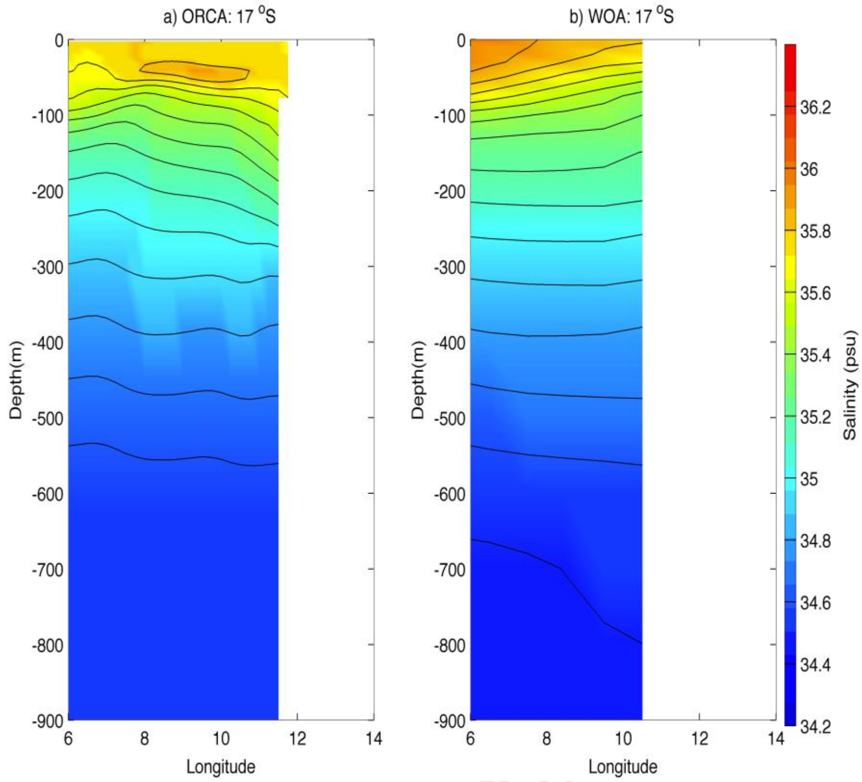

Figure 4.4: salinity section validation between a) ORCA -025 (annual mean) and b) WOA at 17 °S.

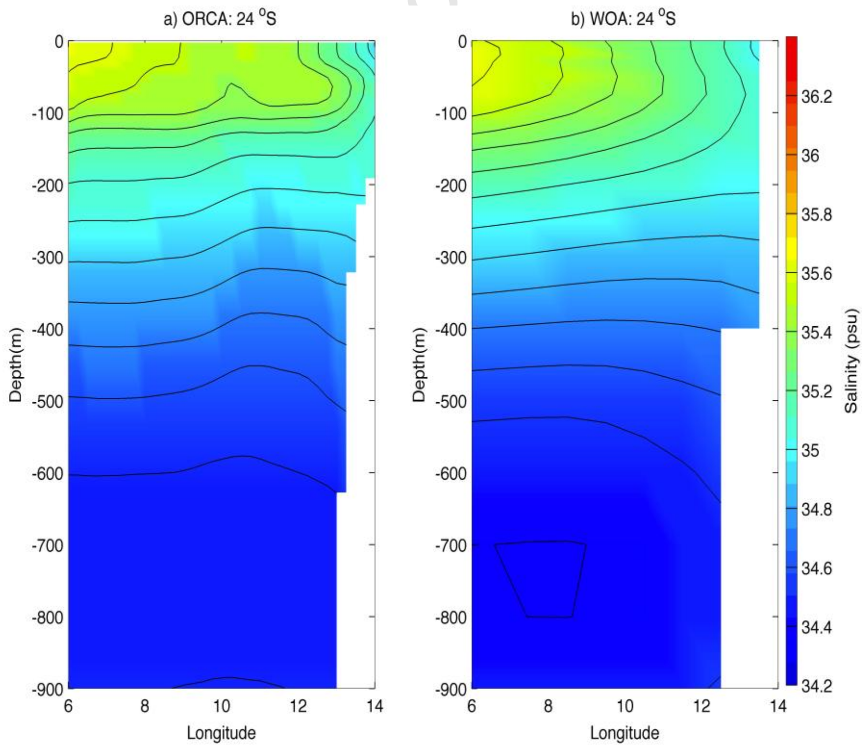

Figure 4.5: salinity section validation between a) ORCA -025 (annual mean) and b) WOA at 24 °S.

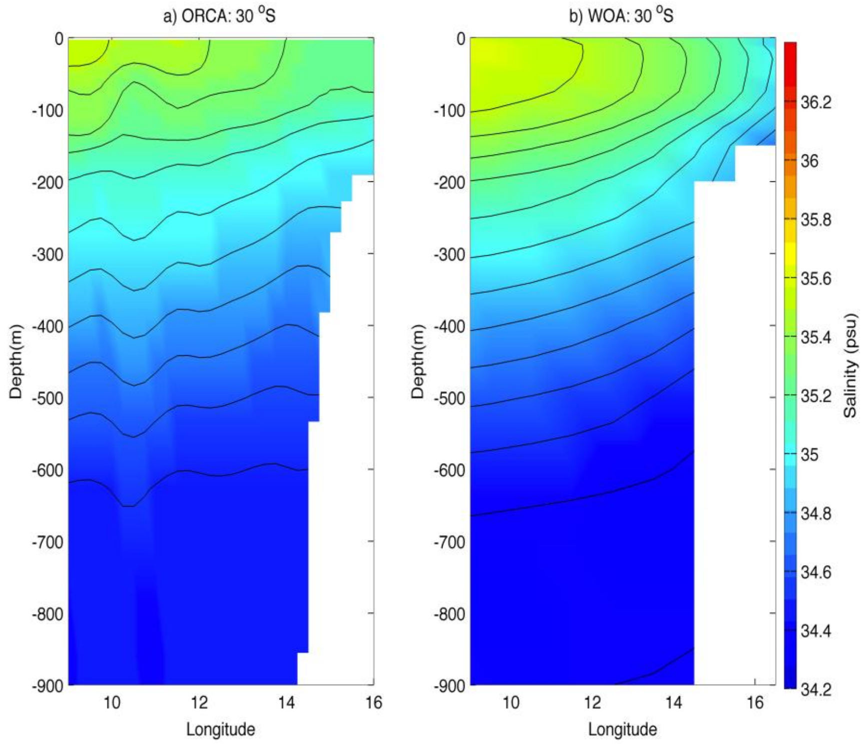

Figure 4.6: salinity section validation between a) ORCA -025 (annual mean) and b) WOA at 30 °S.

4.1.2 Annual mean

The annual mean meridional velocity transects show the PUC at each latitude, 17 °S, 20 °S, 24 °S, 27 °S and 30 °S (Figure 4.7, 4.8, 4.9, 4.10 and 4.11). In the northern Benguela, current is faster moving (~ -0.06 to -0.04 $m.s^{-1}$), whereas at 27 °S and 30 °S the current becomes slower (~ -0.02 to 0 $m.s^{-1}$). The transects clearly show the PUC associated with the Sverdrup relation increasing in depth and widens as it moves further south.

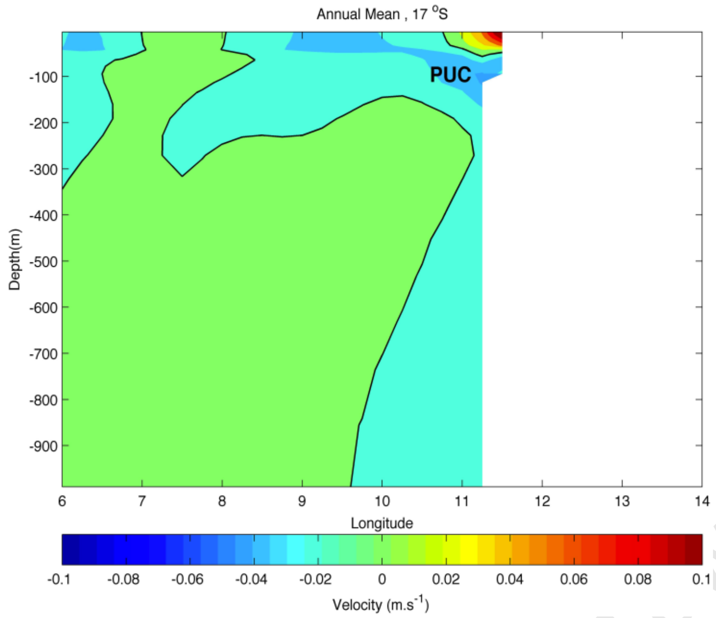

Figure 4.7: annual mean meridional velocity transect at 17 °S. PUC=Poleward Undercurrent.

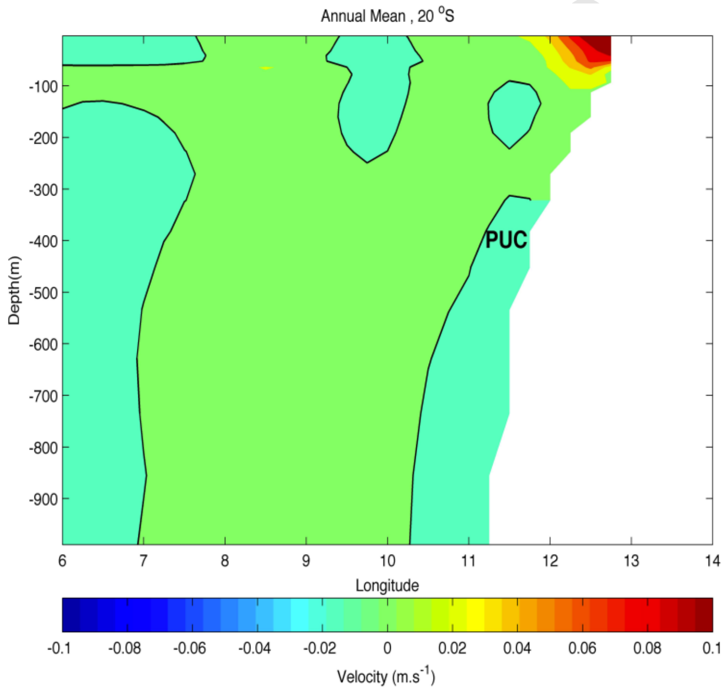

Figure 4.8: annual mean meridional velocity transect at 20 °S. PUC=Poleward Undercurrent.

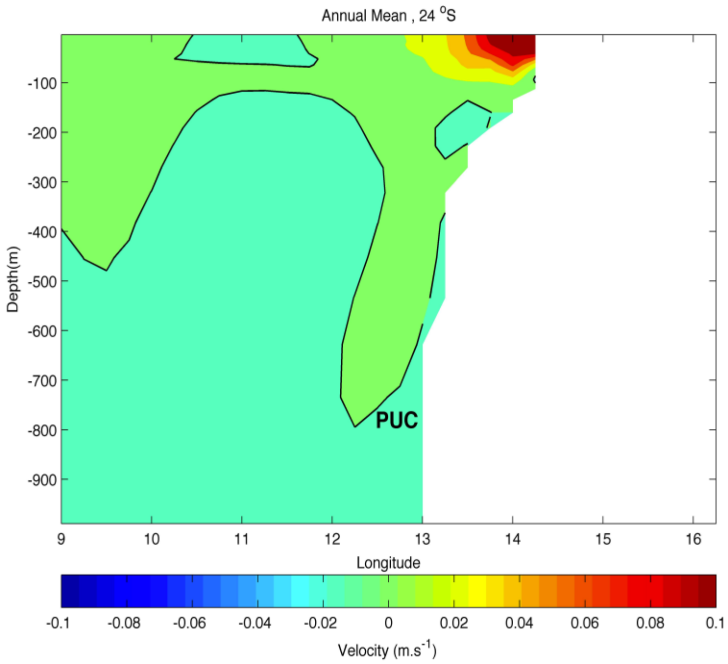

Figure 4.9: annual mean meridional velocity transect at 24 °S. PUC=Poleward Undercurrent.

At 17 °S the PUC is fast moving and apparent, whereas at 20 °S the PUC has become less obvious and suggests intermittent flow at that latitude. At 17 °S it has a core depth of 100 m and by the time it reaches 30 °S it has a core depth of 700 m. At 24 °S, 27 °S and 30 °S the PUC widens, deepens and decreases in velocity (~ -0.02 to 0 $m.s^{-1}$). The figures (figure 4.7, 4.8, 4.9, 4.10, 4.11) show how the PUC follows the shelf-edge moving south. The PUC at 24 °S and 27 °S indicates that the shallow velocities of the current has moved away from the shelf-edge, whereas at 30 °S the current returns to hugging the shelf–edge. The poleward undercurrent can be positioned more offshore and may reach the sea surface and the surfacing of the undercurrent is seawards of the coastal jet (Fennel et al., 2012). The east-west velocities at pertinent locations were looked at to understand the offshore movement of the PUC as it moves southward. At 24 °S and 27 °S there is more offshore flow from the PUC, which may be a result of the shallow velocities detaching from the shelf-edge.

The monthly climatologies (see Appendix) were calculated of the PUC at each transect. The monthly climatologies showed that the peak velocity months are December, January and February. The monthly climatologies also show peak months of velocity in March, April and May. The peaks seen during these months, is the PUC is associated with the upwelling regime. This pattern is represented at each of the transects, however, the magnitude of difference between the different months becomes less apparent at 24 °S, 27 °S and 30 °S (see Appendix).

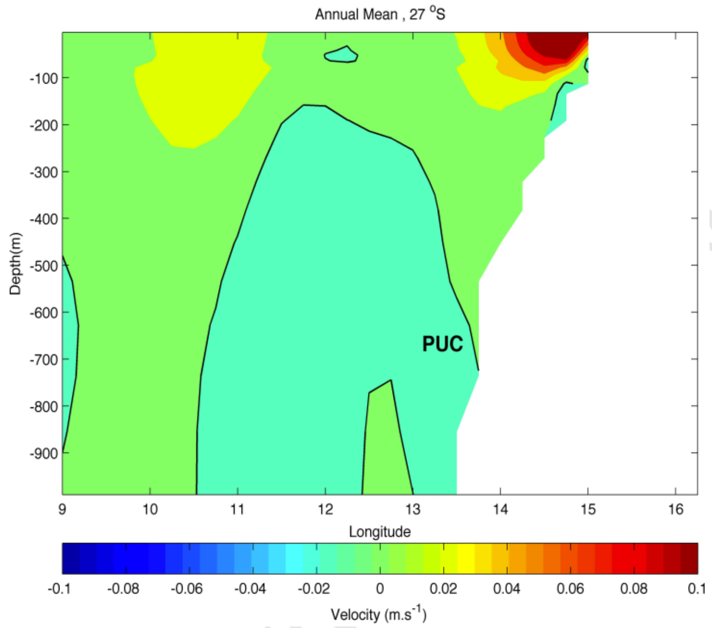

Figure 4.10: annual mean meridional velocity transect at 27 °S. PUC=Poleward Undercurrent.

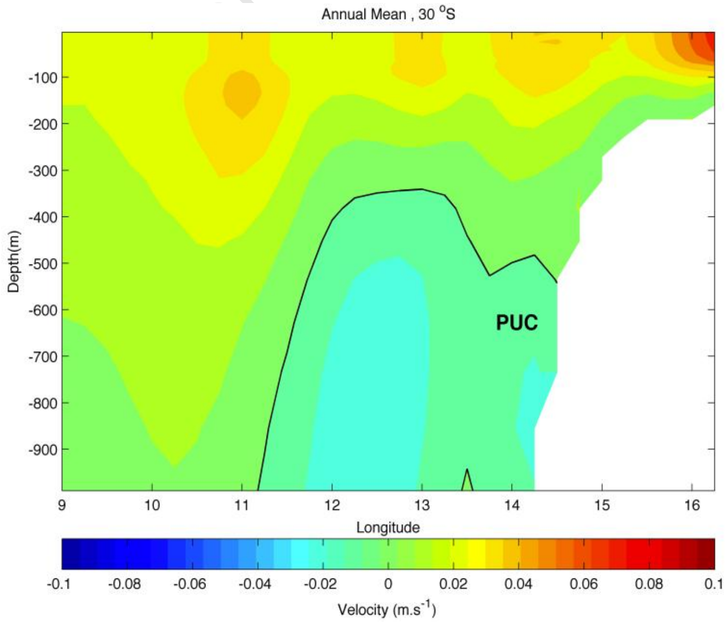

Figure 4.11: annual mean meridional velocity section at 30 °S. PUC=Poleward Undercurrent.

An assessment was made of the PUC core water mass characteristics at each of the transects. The water mass characteristics comparisons were completed by looking at annual mean temperature-salinity plots (figures 4.12, 4.13, 4.14 and 4.15) at each transect. At 17 °S the PUC has a core depth of ~150 m with a temperature of 13.5 °C and a salinity of ~35.28 psu. By 20 °S, the core depth is ~200 m with a temperature of ~12.3 °C and salinity of ~35.17 psu. When the core depth of the PUC reaches ~250 m at 24 °S, the temperature has dropped to ~10.1 °C and exhibits a salinity of ~34.9 psu. When the PUC reaches a depth of ~600 m the temperature is ~5.2 °C and salinity is ~34.48 psu. At 30 °S the core depth of the PUC is at ~700 m, with a temperature of ~4.5 °C and salinity of ~34.45 psu. As the PUC deepens moving south, the temperature decreases, as does the salinity. The cooler temperatures and decreasing salinities are representative of the core of the PUC increasing in depth. In the northern Benguela there is a high core salinity, which is representative of the AAIW mass from the Angola Basin entering the Benguela region by means of the PUC (Shillington et al., 2006). In the north the SACW (LOW) is advected by the PUC, LOW is only found down to Luderitz (~27 °S) (Monteiro & van der Plas, 2006), whereas further south AAIW is transported. The high salinities along the shelf-edge are consistent with the PUC Angola Basin origin (Shillington et al., 2006).

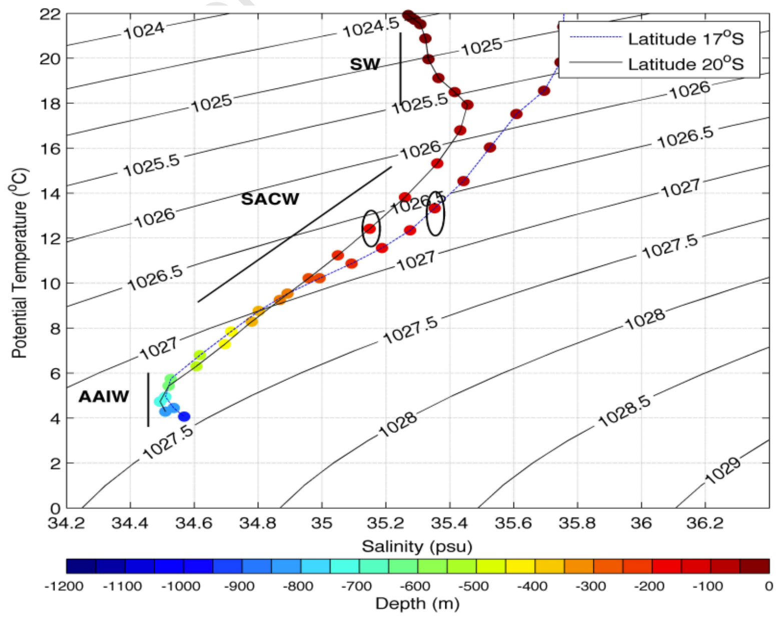

Figure 4.12: annual mean temperature-salinity plot comparing 20 °S with 17 °S. Black circles indicate core of PUC at each latitude. AAIW=Antarctic Intermediate Water, SACW=South Atlantic Central Water, SW=Surface Water.

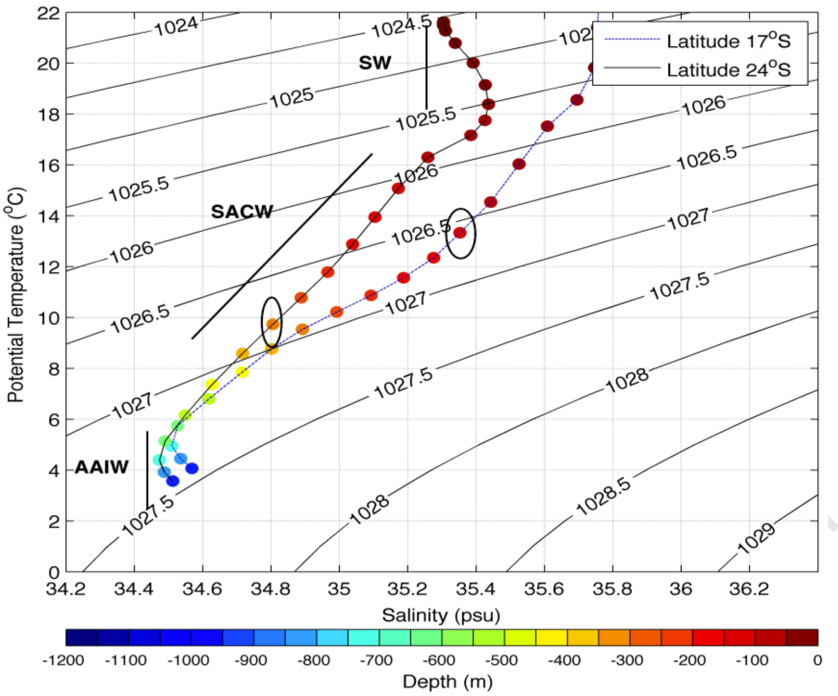

Figure 4.13: annual mean temperature-salinity plot comparing 24 °S with 17 °S. Black circles indicate core of PUC at each latitude. AAIW=Antarctic Intermediate Water, SACW=South Atlantic Central Water, SW=Surface Water.

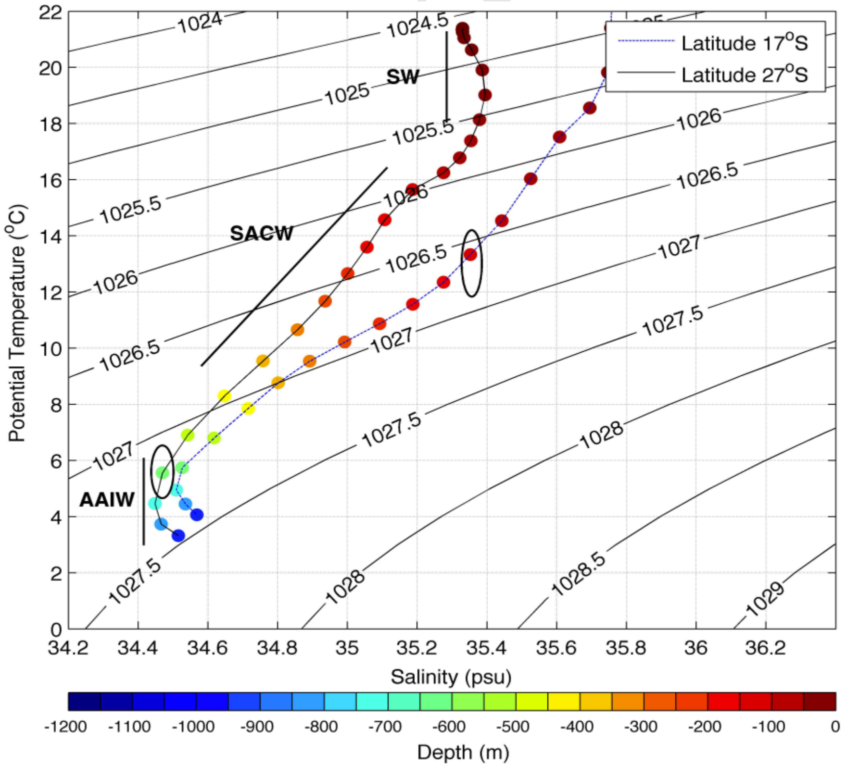

Figure 4.14: annual mean temperature-salinity plot comparing 27 °S with 17 °S. Black circles indicate core of PUC at each latitude. AAIW=Antarctic Intermediate Water, SACW=South Atlantic Central Water, SW=Surface Water.

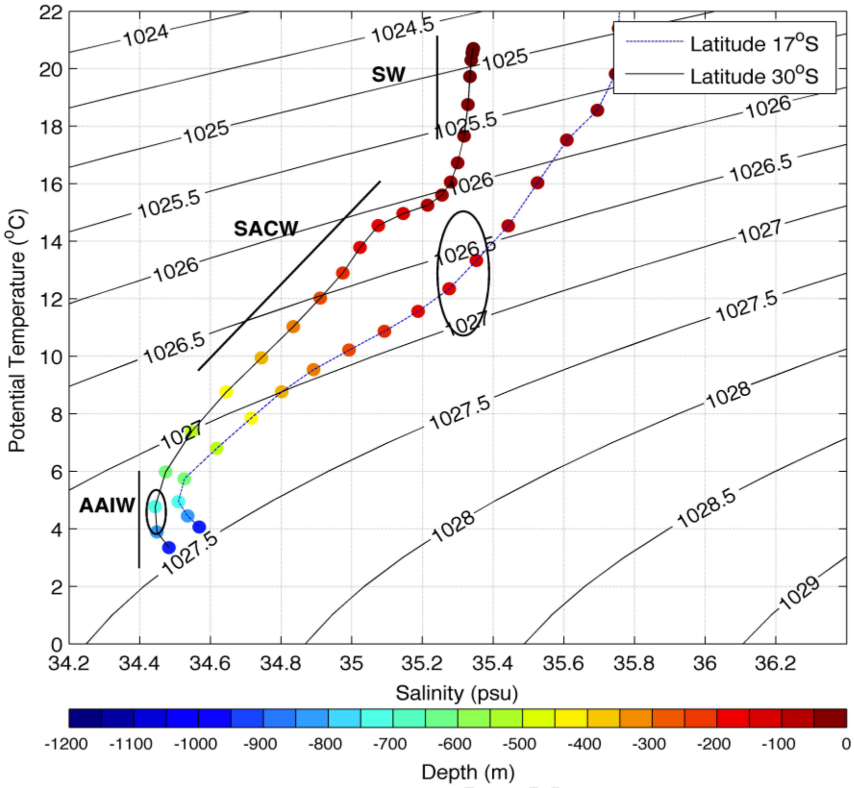

Figure 4.15: annual mean temperature-salinity plot comparing 30 °S with 17 °S. Black circles indicate core of PUC at each latitude. AAIW=Antarctic Intermediate Water, SACW=South Atlantic Central Water, SW=Surface Water.

4.1.3 Seasonality

The seasons were assigned accordingly; summer (December, January, February), autumn (March, April, May), winter (June, July, August) and spring (September, October, November). Figure 4.16 shows the meridional velocities of the PUC stream associated with the Sverdrup relation to be stronger during the austral summer and early autumn. As one moves southwards the PUC becomes much weaker. During winter the PUC becomes weaker at each transect because of the meridional flow of the Benguela Current is largely northwards and intensifying (Mohrholz et al., 2008). During winter and early spring the PUC may become intermittent, which can be seen at 17 °S and 20 °S in figure 4.16 and figure 4.17. At 24 °S, 27 °S and 30 °S (Figure 4.18, figure 4.19 and figure 4.20 respectively) the current is more persistent, however, the strength of the current during winter and early spring remains weaker than in summer and autumn. At 20 °S (figure 4.17), the PUC is shallow and shows a stronger current in summer and autumn. During those months the maximum velocities reach -0.08 to -0.1 $m.s^{-1}$. In June, July, August and September, October, November the current is weaker with maximum velocities only reaching -0.04 to -0.06 $m.s^{-1}$. At 20 °S (Figure 4.17), the PUC is weaker compared to the current at 17 °S, however, the current is stronger during summer and autumn with velocities reaching -0.04 to -0.06 $m.s^{-1}$.

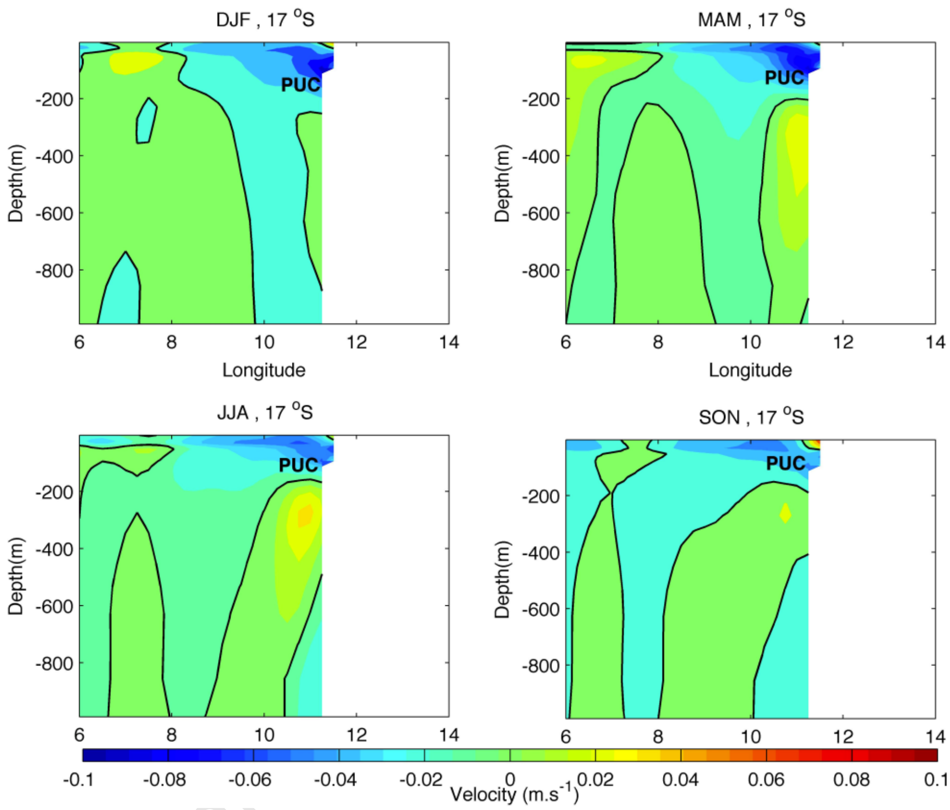

Figure 4.16: meridional seasonal mean velocities at 17 °S (bold = 0 $m.s^{-1}$). PUC=Poleward Undercurrent.

In figure 4.18, showing the PUC at 24 °S, the PUC is more noticeable than at 20 °S, with higher velocities in summer in autumn, but the higher velocities only reach -0.02 to -0.04 $m.s^{-1}$. At 27 °S the PUC shows the same seasonality as the preceding transects with higher maximum velocities of -0.07 $m.s^{-1}$. The PUC at 27 S shows the highest difference in seasons with a value of -0.05 $m.s^{-1}$. At 30 °S, there is more southward flow during summer and autumn and during the winter and spring the PUC shows spatially less southerly meridional velocities.

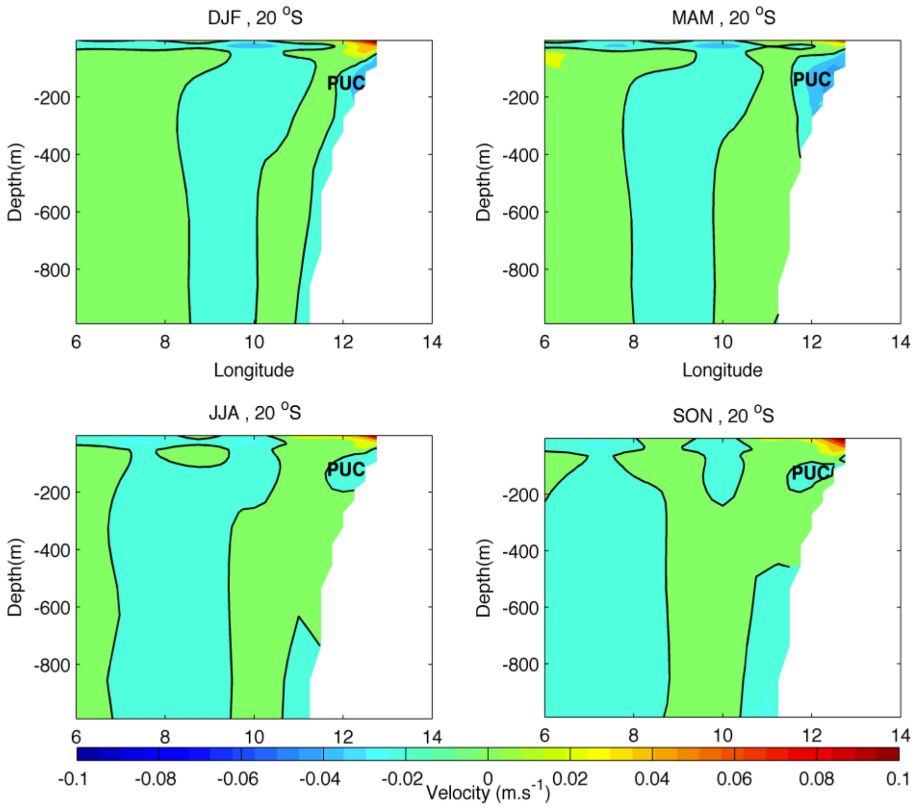

Figure 4.17: meridional seasonal mean velocities at 20 °S (bold = 0 m.s^{-1}). PUC=Poleward Undercurrent.

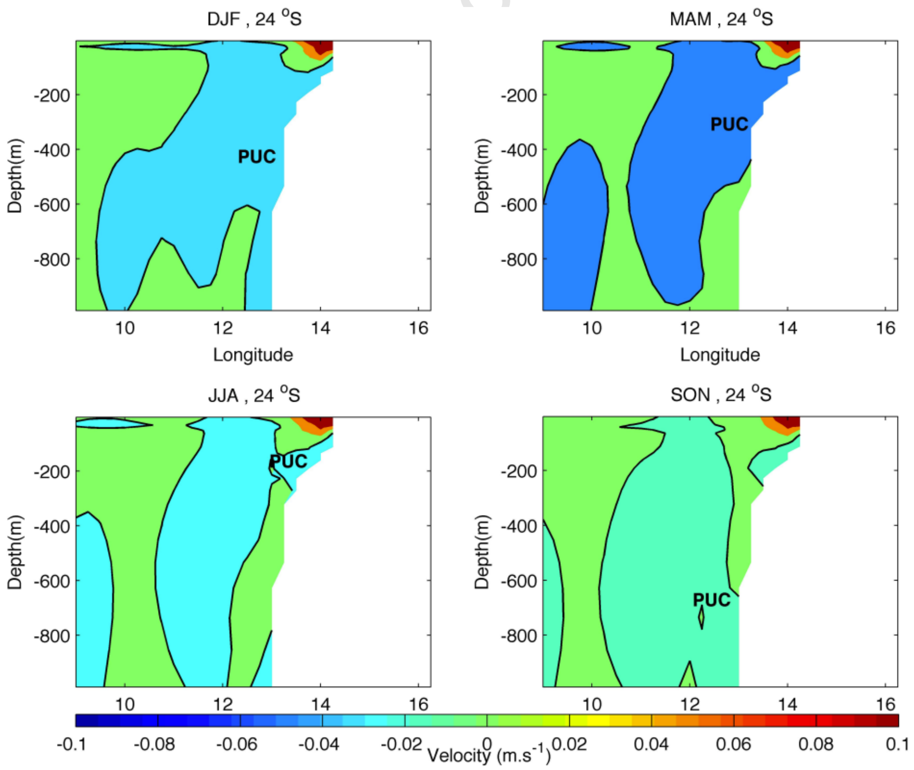

Figure 4.18: meridional seasonal mean velocities at 24 °S (bold = 0 m.s^{-1}). PUC=Poleward Undercurrent.

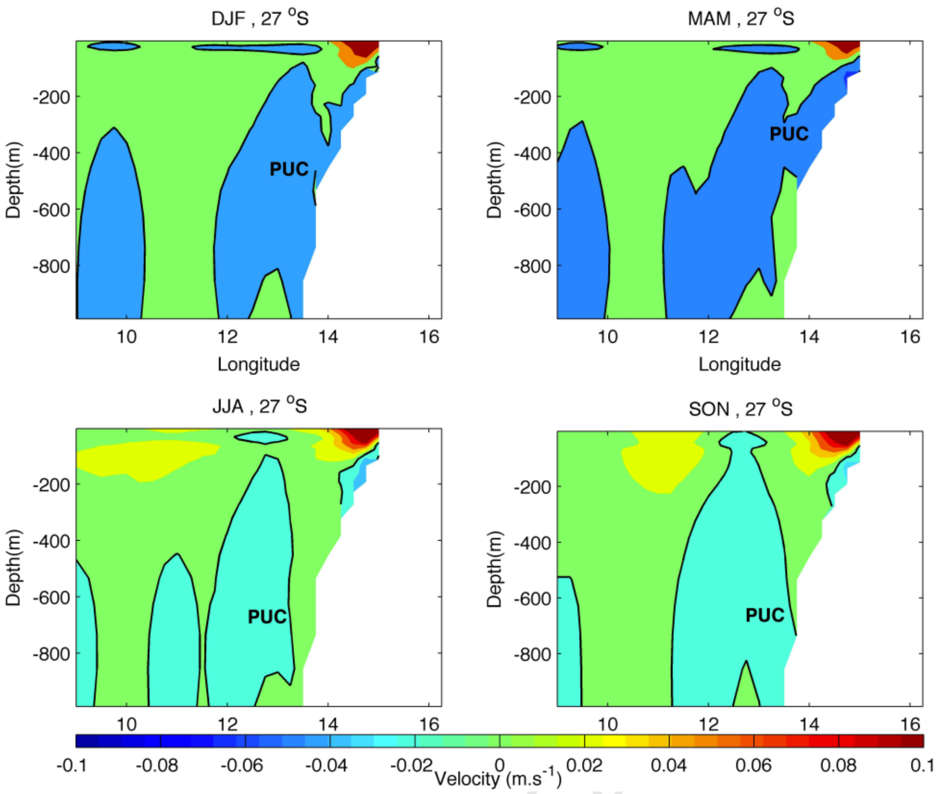

Figure 4.19: meridional seasonal mean velocities at 27 °S (bold = 0 $m.s^{-1}$). PUC=Poleward Undercurrent.

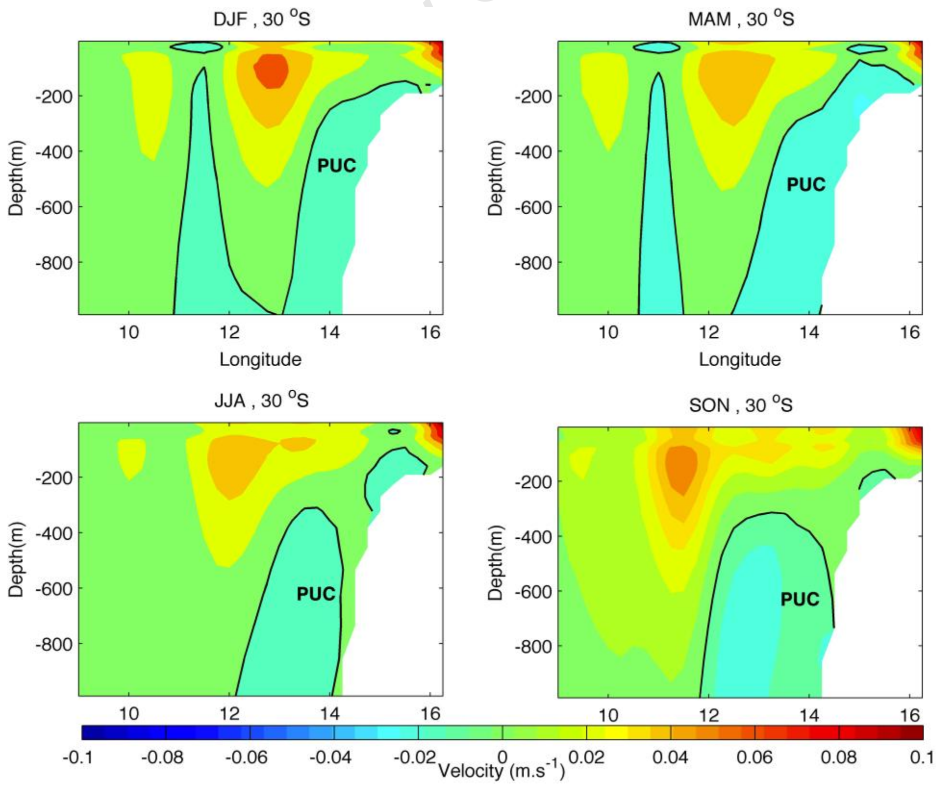

Figure 4.20: meridional seasonal mean velocities at 30 °S (bold = 0 $m.s^{-1}$). PUC=Poleward Undercurrent.

According to Mohrholz et al. (2008), LOW peaks in June to August. The seasonal velocities do not agree with the LOW peaks, however, there is agreement with the monthly southward transports and LOW peaks (figure 4.21). Integrating only the negative velocities at each transect (T1 – T2 from 6 °E – 14 °E; T3-T5 from 9 °E – 16 °E) and multiplying by the change in depth (0-1000 m) with change in longitude to calculate the transports. The negative velocities were only taken into account because they represent the southward flow of the PUC. The monthly transports at each section show the highest transport in June, July, August and September. The lowest transport occurs during March, April, May and November. At 17 °S the southward transport is the highest (with variance 0.7964). At the other transects the southward monthly transports are similar, with transport at 20 °S being lowest during March, April and May (with variance of 0.6751). At 24 °S, 27 °S and 30 °S have monthly transports with the least variance (0.4793, 0.4677, 0.6274 respectively) from the mean. In the austral summer there is the presence of LOW transported by the PUC from the Angola Dome to the central Namibian shelf (Mohrholz et al., 2008). The strength of the PUC determines the occurrence of anoxic waters in the northern Benguela region (Mohrholz et al., 2008). The peaks and known presence of LOW is commensurate with the seasonal peaks of the PUC at each of the transects.

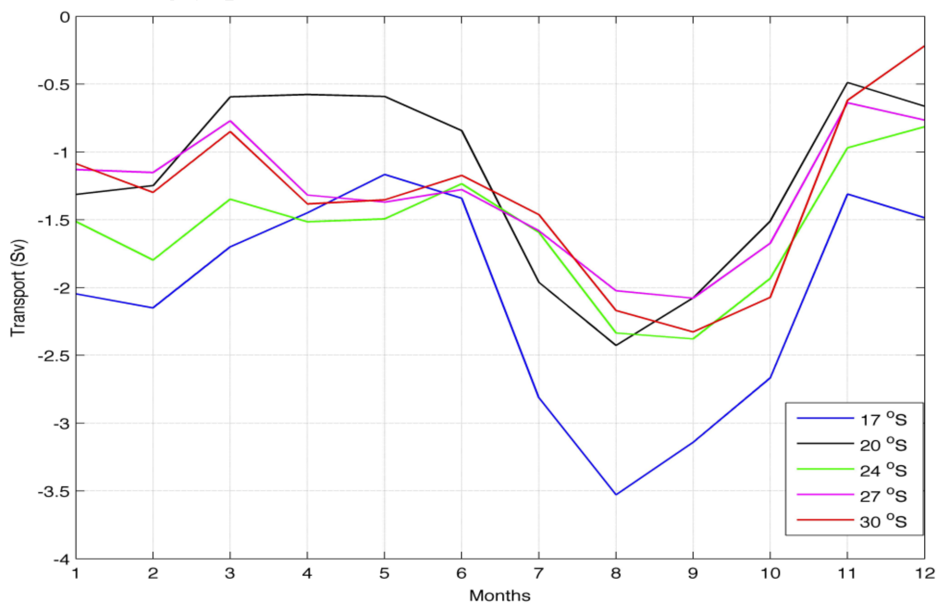

Figure 4.21: monthly climatologies of southward transport at each transect.

4.1.4 Interannual variability

The interannual variability was explored by looking at the southward transport at each transect. Figure 4.22 shows the normalized positive and negative anomalies calculated from the mean of southward transport from 1979 to 2004. Dividing the anomalies by the standard deviation at each transect normalized the anomalies. The normalized anomalies provide a clearer representation of the anomalies. The positive anomalies of transport indicate weaker southward flow and negative anomalies indicate stronger southward transport. The transport anomalies at 17 °S seem to have a more seasonal signal compared to the other transects. At 17 °S the most significant negative transport anomalies (= -2 standard deviation) occurred in 1982, 1989 and 1991. The anomalies at 17 °S are of lower magnitude compared to the anomalies at the other latitudes. At 20 °S peak negative transport anomalies (≥ -2 standard deviation) occurred in 1982, 1994 and 2000. The significant negative transport anomalies (≥ -2 standard deviation) at 24 °S were from 2003 – 2004. The transport is greater at 27 °S and 30 °S than at 17 °S, 20 °S and 24 °S. The peak negative transport anomalies (≥ -2 standard deviation) at 27 °S occurred in 1991 – 1992 and 1994 -1995. At 30 °S with a peak negative transport anomalies (= -2 standard deviation) were in 1991, 1997 and 2001. The positive anomalies at each transect never reach 2, indicating that the PUC shows greater negative anomalous years when the transport is elevated.

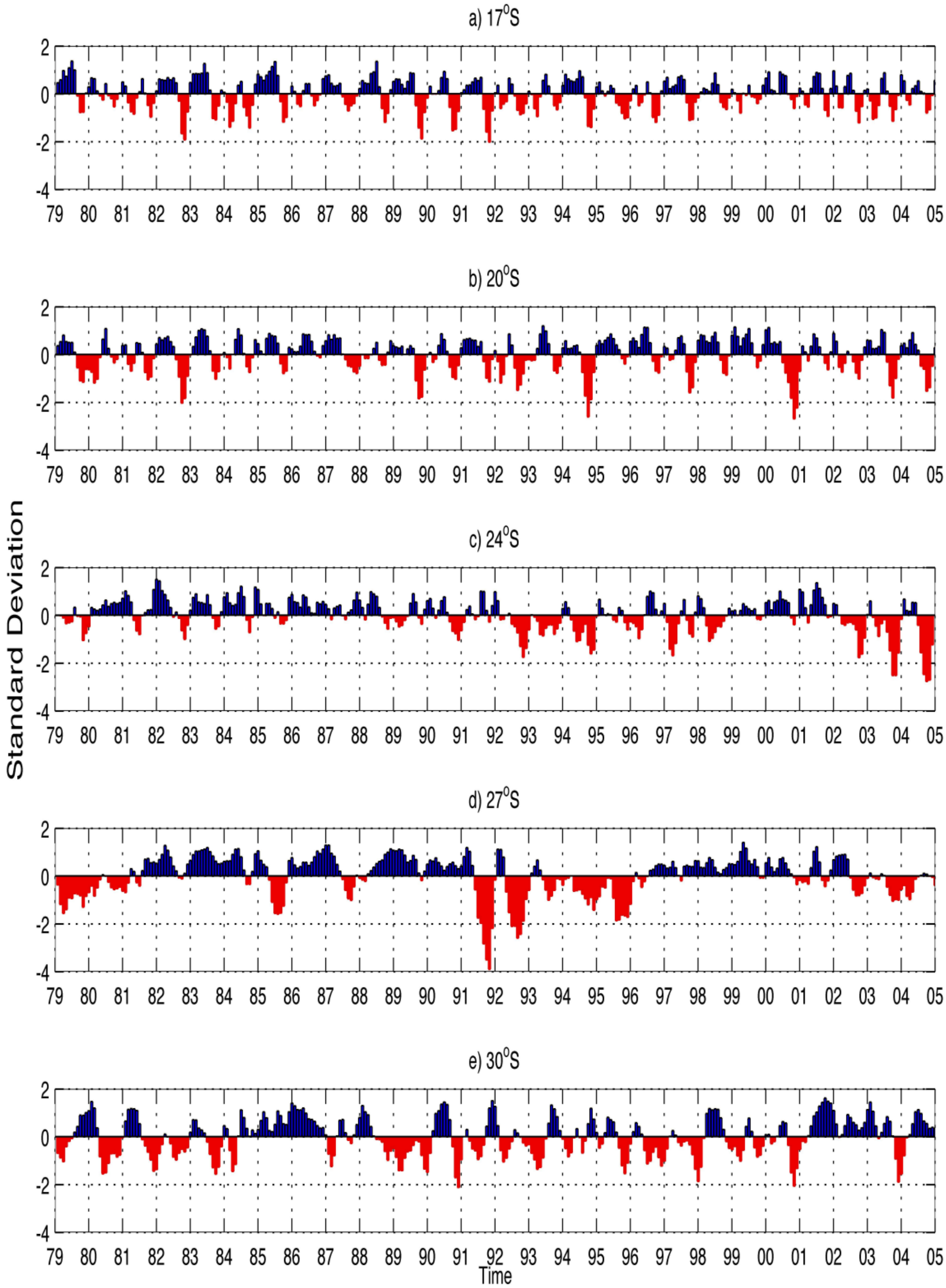

Figure 4.22: normalized anomalies of southward transport (Sverdrup) at a) 17 °S, b) 20 °S, c) 24 °S, d) 27 °S and e) 30 °S from 1979 to 2004.

4.1.5 Atmospheric control

A correlation was made between the normalized anomalies at each transect with Nino 3.4. The Nino 3.4 index was taken from Climate Explorer (http://climexp.knmi.nl) and compared with transport anomaly model data. The correlation with no lag at each of the transects, however, the correlation did not yield any significant similarities between the normalized anomalies and Nino 3.4. Other lag times were explored, but resulted in no significant relation.

The wind stress curl was explored to see if there is a relationship with the southward transport. Figure 4.23 shows the monthly climatologies of wind stress curl at each transect. At 17 °S the wind stress curl is negative from January to May and July to December, with positive wind stress curl in June. The peak wind stress curl at 17 °S is > -2 $N.m^{-3}$. The wind stress curl at 20 °S shows less negative wind stress curl than at 17 °S, 24 °S, 27 °S and 30 °S. At 24 °S and 27 °S the peak negative wind stress curl (> -1 $N.m^{-3}$ and 1 $N.m^{-3}$ respectively) occurs in August. At 30 °S the wind stress curl is positive from April to September. The wind stress curl at 30 °S shows a different signal compared to the other transects, as the wind regime at 30 °S illustrates a different seasonal cycle to the northern Benguela.

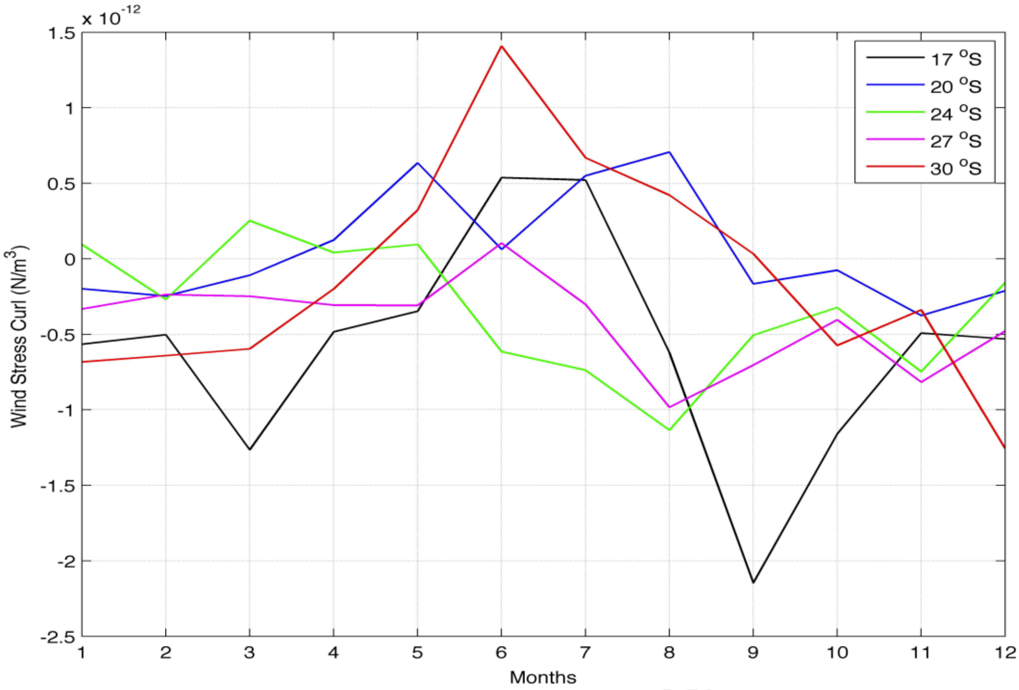

Figure 4.23: monthly climatologies of wind stress curl (N/m^3) averaged across each transect.

Figure 4.24 represents the monthly mean wind stress curl normalized anomalies from 1979 to 2002. The positive anomalies indicate a more positive wind stress curl or less negative wind stress curl and the negative anomalies indicate a more negative wind stress curl. The focus will be on the negative wind stress curl anomalies, as it is the negative (cyclonic) wind stress curl that drives the relationship with the PUC (Veitch et al., 2010). The significant anomalies are distinguished by a value of more than 3. At 17 °S the significant negative wind stress curl anomalies (> 4 standard deviation) occurred in 1980 and 1997. The significant negative anomalies (= 5 standard deviation) occurred in 1997 and positive anomalies in 1994, 1995 and 1998 (>4 standard deviation), at 20 °S. At 24 °S it does not show many significant negative wind stress curl anomalous years except for 1982 and 1995 (> 3 standard deviation) and positive anomalies in 1998 (>4 standard deviation). Significant negative anomalies of > 4, are seen 1983, 1989, 1990 and 2000 at 27 °S. The negative wind stress curl anomalies at 30 °S are weaker than at 27 °S, however, at 1979, 1992 and 1998 there are anomalies of >3.

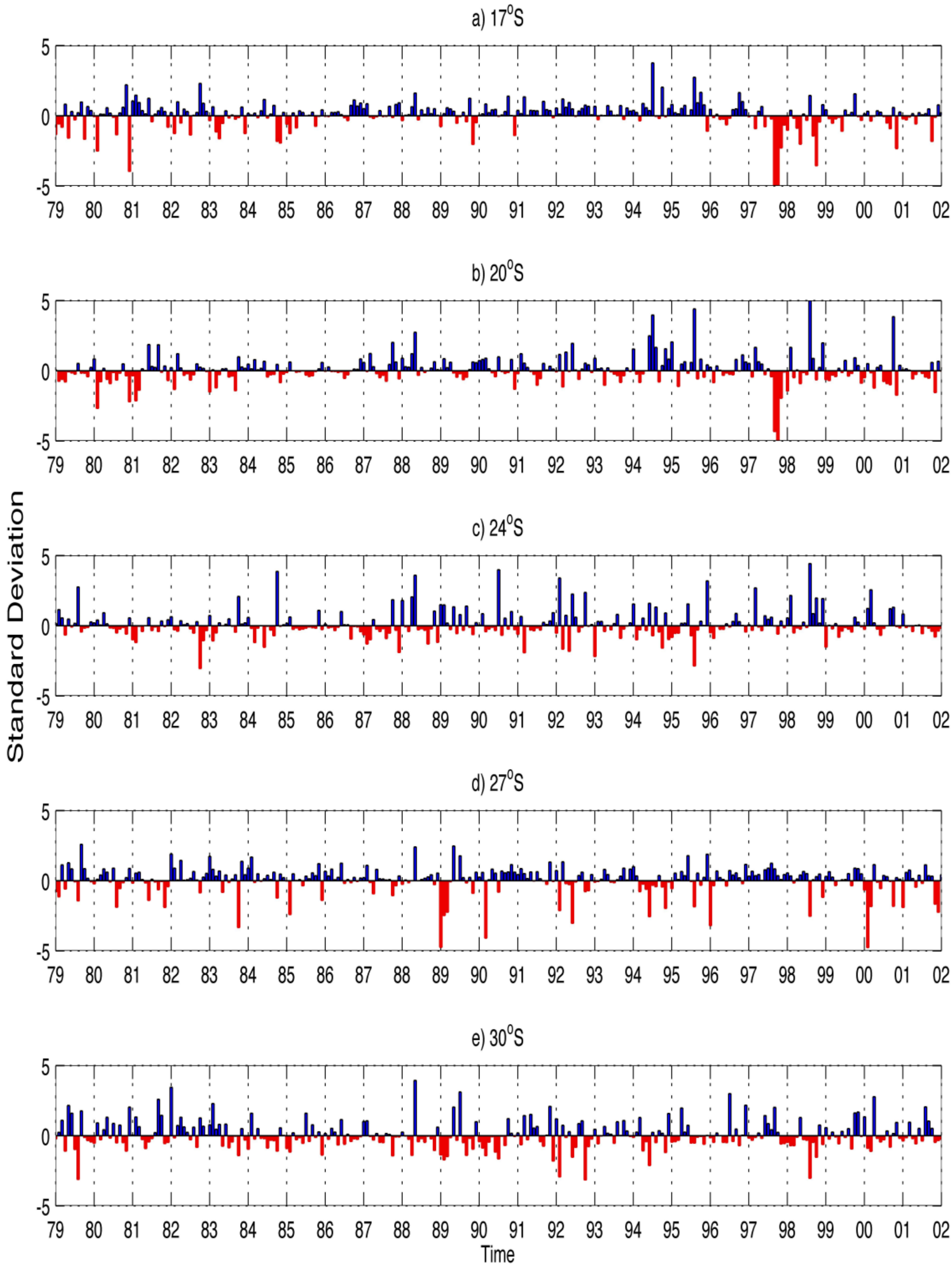

Figure 4.24: normalized anomalies of monthly mean wind stress curl from 1979 to 2002.

5. Discussion

The dynamics of the PUC in the Benguela system has been addressed with the use of ORCA-025 model. The model has provided an opportunity to study the PUC associated with the Sverdrup relation spatially and temporally in the Benguela system. The simulation of the PUC has allowed the exploration of the seasonal and interannual variability of this current, including the characteristics of the PUC.

In figure 4.2 there is a phase shift of one month between the model and OI SST. The model depicts the peak of the phase to be one month earlier than the OI SST data. It is likely that the model is incorrect as it has a low resolution to resolve the intensity of the front. As a result the model will produce an average higher temperature in that region. As seen in figure 4.2 the model also undermines the upwelling regime, it does not properly resolve the upwelling and front, which is why it is generally warmer. The phasing is a month earlier in the model not because of the upwelling as the upwelling favorable winds are accurate but possibly it is not correctly resolving the warm pulsing coming from the north (i.e. the Angola Current). The model shows extreme SST values in the years 1984 and 1995 (Figure 4.3). The reason for this may be that the model is picking up the increased SST signal from the Benguela Niño events. The strongest Benguela Niño events are not reflected in the transport anomalies. This may be because the transport is on the surface above the thermocline and it is masked with integrating transport with depth. Or that it is being masked by the strong equatorward flow at the bottom and calculating transport a long way offshore (transport signal is hidden by integrating over a large domain) (Molines et al., 2007).

5.1 General characteristics

The model ORCA-025 simulated the presence of the PUC from 17 °S to 30 °S. At each transect for velocity (Figures 4.7, 4.8, 4.9, 4.10 and 4.11) the model clearly shows the PUC along the shelf-edge. The velocity transects show the PUC to be considerably stronger in the most northern transects and decreasing in strength moving south. The decreasing velocity of the current moving south may be related to the cross-shore velocities, particularly at the Luderitz upwelling cell. Between ~25 °S-27 °S, a considerable amount of the poleward flow veers offshore due to the nature of the wind stress curl and its interaction with the northwestward path of the Benguela Current (Veitch et al., 2010). After the Luderitz cell the PUC becomes weaker. The poleward flow deepens as it moves south (especially between 24 °S and 30 °S), due to a substantial amount of flow that veers offshore due to the wind stress curl and its interaction with the northwestward path of the Benguela Current (Veitch et al., 2006). Where there is an undercurrent, there is weak downwelling below the core and the presence of the shelf weakens the current (Julian et al., 1985), supported by the findings of the velocity transects. The velocity transects show how the topography in the Benguela region controls the path and momentum of the PUC (Mooers, 1989).

Table 5.1 provides a summary of the PUC characteristics. In the northern Benguela the PUC is ~ 55 km offshore, reaching ~220 km offshore at 30 °S. At 17 °S the pace of the current is faster than at the other transects with a maximum velocity of -0.1191 $m.s^{-1}$. By 20 °S the current has slowed to a maximum rate of -0.0818 $m.s^{-1}$, with a slight increase at 24 °S at a rate of -0.0945 $m.s^{-1}$. At 27 °S and 30 °S, the current rate decreases further with a rate of -0.0374 $m.s^{-1}$ and -0.0356 $m.s^{-1}$ respectively. The average velocity at each transect show a similar pattern with the highest rate at 17 °S of -0.0362 $m.s^{-1}$, decreasing to -0.0289 $m.s^{-1}$ at 20 °S, with a slight increase at 24 °S at a rate of -0.0299 $m.s^{-1}$. The current average velocity decreases at 27 °S to -0.0137 $m.s^{-1}$ and -0.0110 $m.s^{-1}$ at 30 °S. Veitch et al. (2010), suggests that the alongshore velocities of the poleward flow do decrease moving southwards with a slight increase at ~23 – 24 °S.

The water mass characteristics of the PUC shown in table 5.1 depict changes in temperature and salinity as the current moves south. The water mass of the PUC is AAIW, which has a salinity minimum deep in the water column in the northern and southern Benguela (Shillington et al., 2006). In the northern Benguela along the shelf-edge there is a salinity minimum associated with the core of AAIW mass, which has a salinity of 34.5- 35.6 psu at 400 – 650 m. A high salinity AAIW from the Angolan Basin enters the northern Benguela region via the PUC along the shelf – edge

(Shillington et al., 2006). The southern Benguela has a low salinity AAIW (Shillington et al., 2006), which is shown by the model where in the north the PUC has a salinity of ~35.28 psu and decreases to ~34.45 psu in the south.

Characteristics	17 °S	20 °S	24 °S	27 °S	30 °S
Offshore location (km)	~55	~110	~170	~220	~220
Core depth (m)	~150	~200	~250	~600	~700
Peak velocity ($m.s^{-1}$)	-0.1191	-0.0818	-0.0945	-0.0374	-0.0356
Average velocity ($m.s^{-1}$)	-0.0362	-0.0289	-0.0294	-0.0137	-0.0110
Transport (Sv)					
Summer	-1.90	-1.08	-1.39	-1.01	-0.87
Autumn	-1.4	-0.6	-1.45	-1.17	-1.2
Winter	-2.6	-1.77	-1.73	-1.62	-1.6
Spring	-2.4	-1.38	-1.78	-1.48	-1.67
Variance	0.5042	0.4871	0.1919	0.28	0.3756
Core salinity (psu)	~35.28	~35.17	~34.90	~34.48	~34.45
Core temperature (°C)	~13.5	~12.3	~10.1	~5.2	~4.5

Table 5.1: table of PUC general characteristics.

5.2 Variability

The results show the PUC is faster flowing in austral summer and autumn and becomes weaker in winter and spring. It has been shown that the maximum southward penetration into the northern Benguela region is during the late summer and early autumn, which coincides with the intensification of the Angolan Current and partial relaxation of the equatorward wind stress along the Namibian coast (Hardman-Mountford et al., 2003). The seasonal figures (4.16 to 4.20) correspond with this finding. Figures 4.16 to 4.20 show the PUC to be stronger during summer and autumn, with slower moving PUC during the rest of the year. The PUC is influenced by the topography, so the intermittent PUC seen during the winter and spring in figures 4.16 and 4.17 at 17 °S and 20 °S may be influenced by the Walvis Ridge (at ~20 S), which may have an effect on a continuous alongshore flow (Mooers, 1989).

The seasonal transport of the PUC shows peaks in winter and spring and decreases in summer and autumn. The negative wind stress curl peaks in winter and spring, which is commensurate with the seasonal transport. The negative wind stress curl drives the transport of the PUC via the Sverdrup relation (Veitch et al., 2010), which is seen in similar peaks in wind stress curl and transport. The differences in seasonal peaks for velocities and transport may be a result of weaker velocities over a larger area and the PUC changes spatially with all negative transports integrated across each transect. The southward transport anomalies and wind stress curl anomalies do not depict the strongest Benguela Niño events in 1984 and 1995, however, the more significant anomalies coincide with years of Benguela Niño events. This may be because the model is not suitable to reproduce these events or these events are not driven by the southward SACW advection but extreme heat fluxes at the sea surface (Risien & Chelton, 2008).

The wind stress curl peak anomalous years do not show a relationship with ENSO events. The peak wind stress curl anomalous years that correspond to Benguela Niño warm event years were 1984, 1991, 1994 – 1995 and 1997 – 1998 and cold event years were 1983, 1991 – 1992 and 1996 - 1997 (Rouault et al., 2010). The peak wind stress curl anomalous years and peak transport anomalous years do illustrate a relationship. The peak anomalous years of wind stress curl at each transect correspond to certain Benguela Nino events; at 17 °S (1997), at 20 °S (1994 – 1995), at 24 °S (1995), at 27 °S (1983) and at 30 °S (1992). The wind stress curl is the driving force of the PUC, which relates to the transport of the PUC. An increase in wind stress curl is likely to result in increased transport in the PUC. The PUC transport relies on the wind stress curl seasonally and interannually.

The poleward progression of LOW progresses in summer (Nelson, 1989). According to Mohrholz et al., (2008), in austral summer anoxic conditions are more apparent and observed along the central Namibian shelf brought by the PUC. The strength of the PUC determines the anoxic conditions in the northern Benguela, so during the summer the PUC brings more LOW into the Benguela region and weakens in winter due to the strength of the northward meridional flow (Mohrholz et al., 2008). It is important to know the seasonal variability of the PUC as is it the advection link between the Angola Dome, a reservoir of LOW, and the northern Benguela region (Monteiro & van der Plas, 2006). The LOW is one of the major environmental factors directing the variability and commercial variability of the fisheries and ecosystem along the Namibian coastline, as the PUC is seen to travel the length of the coast (Monteiro & van der Plas, 2006). Evidence was found that there is a bimodal seasonal cycle as well as interannual signals that propagate polewards along the coast from the equatorial region into the Benguela upwelling region (Lass & Mohrholz, 2008). The SACW is advected poleward by the PUC (transporting LOW) with high nutrient content on the shelf of the northern Benguela (Lass & Mohrholz, 2008). The PUC sustains the nutrient balance of the Benguela upwelling but keeps the oxygen concentration of the sub-thermocline water on the shelf on a suboxic level (Lass & Mohrholz, 2008).

The interannual variability was studied by looking at the poleward transport anomalies of the PUC from 1979 to 2004 (Figure 4.22). The magnitude of the southward transport anomalies at 17 °S is less than at the other transects. The peak transport anomalies at 17 °S were in 1982, 1989 and 1991. At 20 °S the highest anomalous years were in 1982, 1994 and 2000. The peak anomalous years at 24 °S were in 2003-2004. At 27 °S the greatest anomalous years were in 1991-1992 and 1995. At 30 °S peak anomalous years were found in 1991, 1997 and 2001. The peak anomalous years at each transect do not correspond to a particular ENSO event, however, Benguela Niños warm events occurred in 1984 (January to June), 1991 (May to June), 1994 -1995 (December to July) and 1997- 1998 (October to January). The cold events occurred in 1983 (February to July), 1991-1992 (November to March) and 1996 – 1997 (October to June) (Rouault et al., 2010). The years of the warm events in 1991, 1994 – 1995 and 1997- 1998 correspond to peak anomalous years at 17 °S (1991), at 20 °S (1994) and at 30 °S (1997). A cold event corresponds to a peak anomaly at 27 °S in 1991- 1992. The seasonal signal in the Atlantic is stronger than the interannual signal (Shannon et al., 1986), which may be an explanation for the sporadic coincidence of peak transport anomalies and Benguela Niño events coinciding. The correlation between the transport anomalies and Nino 3.4 yielded a weak relationship. The transport anomalies of the PUC may not be the key factor in determining a relationship between ENSO and strength of the current.

6. Conclusion

The Benguela system is an upwelling system in the South Atlantic, unique to other eastern boundary systems as two warm water currents bound it – the Angola Current in the north and the Agulhas Current to the south. The northern boundary of the Benguela system is the ABFZ, which is where the Benguela Current and the Angolan Current meet. The Angola Dome to the north of the ABFZ is a source for LOW that is advected southwards via the PUC into the northern Benguela region.

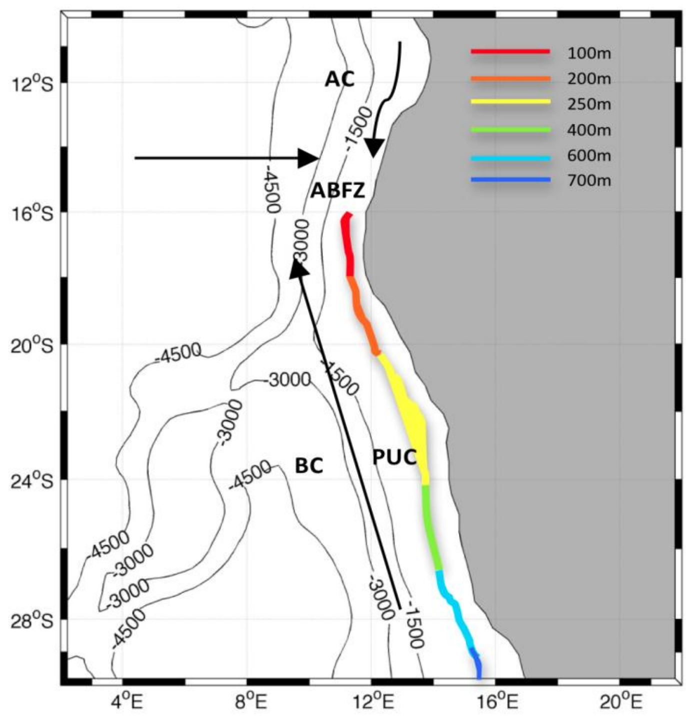

Figure 6.1: schematic of the path and average depth of the PUC (southward flow) along the Namibian coast, Benguela Current (BC), Angola Current (AC) and Angola-Benguela Frontal Zone (ABFZ). The average depth was determined by looking at the core depth of the PUC at each latitudinal interval alongshore and then plotted accordingly.

The model data simulated from ORCA-025 allowed for the examining of the PUC. In the Benguela system there are two PUCs, one that is associated with the upwelling regime and the other is related to the Sverdrup relation. The focus of the study was on the Sverdrup related PUC. The PUC is present from 17 °S to 30 °S with higher velocities in the northern region decreasing in magnitude southwards. The PUC tends to deepen and widen as it moves southwards as it follows the shelf-edge of the Namibian coastline. Figure 6.1 shows how the depth of the PUC deepens moving south. The maximum velocities of the PUC range from -0.1191 m.s-1 in the north to -0.0356 m.s-1 in the south. The PUC is a body of water with AAIW mass characteristics evident at each transect.

The PUC has a seasonal cycle with higher meridional velocities during the austral summer and autumn. The PUC is much weaker in the winter because of the strong meridional northward flow. The strength of the PUC determines the presence of anoxic conditions along the Namibian shelf. The PUC transports LOW from the Angolan Dome into the northern Benguela, which is more prevalent during the summer and autumn. The importance of knowing the seasonality of the PUC is because of the dire effects this current has on marine ecosystems by transporting LOW. The seasonal cycle of the wind stress curl peaks in winter and spring, which corresponds to the peak poleward transports during winter and spring.

The interannual variability of the PUC is less palpable than the seasonal variability. The PUC transport anomalies over the time period 1979-2004 show that there is interannual variability with the coincidence of significant events occurring during Benguela Niño events. The occurrence of Benguela Niños seems to appear where there are significant negative southward transport anomalies in the Benguela system.

In order to grasp a better understanding of the seasonal and interannual variability of the PUC, it would be necessary to explore long-term monitoring of the role of wind stress curl in relation to the PUC. To enable a better understanding of the variability of the PUC, there is a need to continue obtaining *in situ* data, which will improve model outputs for the Benguela region.

Acknowledgments

I am extremely grateful to have had Dr. Mathieu Rouault and Dr. Jennifer Veitch as my supervisors. Their encouragement and support throughout the study were invaluable. The help with the data processing and guidance from Dr. Veitch and Dr. Rouault provided me with an interesting and rewarding experience.

I would like to thank Climate Explorer for the use of Nino 3. 4 correlation data, NOAA_OI_SST_V2 data provided by the NOAA/OAR/ESRL PSD, Boulder, Colorado, USA, from their Web site at http://www.esrl.noaa.gov/psd/ and the DRAKKAR project for the use of ORCA-025 model data.

Finally, I would like to acknowledge the support from ACCESS for funding this project, which otherwise would not have been possible.

References:

Bakun, A. & Nelson, C.S., 1991. The Seasonal Cycle of Wind-Stress Curl in Subtropical eastern Boundary Current Regions. *Journal of the Oceanographical Society of Japan*, 21, pp.1815-1834.

Barton, E.D., 1989. The Poleward Undercurrent on the Eastern Boundary of the Subtropical North Atlantic., pp.82-95.

Barnier B. et al., 2006. Impact of partial steps and momentum advection schemes in a global ocean circulation model at eddy permitting resolution. *Springer, Ocean Dynamics*, Vol. 56 pp. 543-567.

Clarke A. J., 1989. Theoretical understanding of eastern ocean boundary poleward undercurrents. Coastal & Estuarine Studies: Poleward Flows Along Eastern Ocean Boundaries, *Springer-Verlag.* Vol. 34, pp. 17-26.

Climate Explorer [accessed October 2012]: http://climexp.knmi.ni.

Colberg, F. & Reason, C.J.C., 2006. A model study of the Angola Benguela Frontal Zone : Sensitivity to atmospheric forcing. *Geophysical Research Letters*, Vol. 33, pp.6-11.

Colberg, F. & Reason, C.J.C., 2007. A model investigation of internal variability in the Angola Benguela Frontal Zone. *Journal of Geophysical Research Letters*, Vol. 112(C7).

Dingle R. V. & G. Nelson, 1993. Sea-bottom temperature, salinity and dissolved oxygen on the continental margin off southwestern Africa. *South African Journal of Marine Science*, Vol. 13, pp.37-41.

Duncombe Rae, C.M., 2005. A demonstration of the hydrographic partition of the Benguela upwelling ecosystem at 26 ° 40 ' South. *African Journal of Marine Science*, 27(3), pp.617-628.

Fennel, W. & Lass, H.U., 2007. On the impact of wind curls on coastal currents. *Journal of Marine Systems*, 68(1-2), pp.128-142.

Fennel, W., T. Junker, M. Schmidt, V. Mohrholz, 2012. Response of the Benguela upwelling systems to spatial variations in the wind stress. *Continental Shelf Research*, Vol. 45, pp. 65-77.

Gammelsrϕd. T et al., 1998. Intrusion of warm surface water along the Angolan-Namibian coast in February – March 1995 : the 1995 Benguela Nino. *South African Journal of Marine Science*, Vol. 19, pp.37-41.

Giraudeau, J., Bailey, G.W. & Pujol, C., 2000. A high-resolution time-series analyses of particle fluxes in the Northern Benguela coastal upwelling system : carbonate record of changes in biogenic production and particle transfer processes. *Deep-Sea Research*, 47, pp.1999-2028.

Hardman-Mountford, N.J. et al., 2003. Ocean climate of the South East Atlantic observed from satellite data and wind models. *Progress In Oceanography*, 59(2-3), pp.181-221.

Hutchings, L. et al., 2009. The Benguela Current : An ecosystem of four components. *Progress in Oceanography*, 83(June), pp.15-32.

John, H. et al., 2002. ICES CM 2002 Intrusion of Angolan water into the northern Benguela and anomalous cross-slope distributions of fish larvae. *Implications for Biology and Fisheries*, pp.1-15.

John, H.-C. et al., 2004. Oceanographic and faunistic structures across an Angola Current intrusion into northern Namibian waters. *Journal of Marine Systems*, 46(1-4), pp.1-22.

Lass, H.U., et al., 2000. Hydrographic and Current Measurements in the Area of the Angola – Benguela Front. *American Meteorological Society*, 30(1987), pp.2589-2609.

Lass H. U. & V. Mohrholz, (2008). On the interaction between the subtropical gyre and the Subtropical Cell on the shelf of the SE Atlantic. *Journal of Marine Systems,* Vol. 74, pp. 1-43.

McCreary, J.P., 1985. Three-dimensional shelf circulation along an eastern ocean boundary. *Journal of Marine Research*, 43(1976), pp.13-36.

Mohrholz, V. et al., 2008. The seasonal variability of the northern Benguela undercurrent and its relation to the oxygen budget on the shelf. *Continental Shelf Research*, 28(3), pp.424-441.

Molines, J.M. et al., 2007. Definition of the interannual experiment ORCA025-G70, pp.1-34.

Monteiro, P.M.S. et al., 2006. Variability of natural hypoxia and methane in a coastal upwelling system : Oceanic physics or shelf biology? *Geophysical Research Letters,* Vol. 33, pp.1-5.

Monteiro, P.M.S. & van der Plas, A.K., 2006. Low Oxygen Water (LOW) variability in the Benguela System: Key processes and forcing scales relevant to forecasting. *Large Marine Ecosystems*, 14, pp.91-109.

Mooers C.N.K, 1989. Workshop Summary: Poleward Flow- Observational and Theoretical Issues. Coastal & Estuarine Studies: Poleward Flows Along Eastern Ocean Boundaries, *Springer-Verlag.* Vol. 34, pp. 40-46.

Nelson, G., 1989. Poleward Motion in the Benguela Area. Coastal & Estuarine Studies: Poleward Flows Along Eastern Ocean Boundaries, *Springer-Verlag.* Vol. 34, pp. 26-40.

NODC (2009), [accessed November 2012]: http://www.nodc.noaa.gov/OCS/WOA05.

Penven, P. et al., 2005. Average circulation, seasonal cycle, and mesoscale dynamics of the Peru Current System : A modeling approach. *Journal of Geophysical Research.* Vol.110, pp.1-21.

Philander S. G. H. & Yoon, J.H., 1982. Eastern Boundary Currents and Coastal Upwelling. *Journal of Physical Oceanography*, 12, pp.862-879.

Pierce, S.D. et al., 2000. Continuity of the poleward undercurrent along the eastern boundary of the mid-latitude north Pacific. *Deep-Sea Research*, 47, pp.811-829.

Pizzaro O., et al., 2002. Dynamics of seasonal and interannual variability of the Peru-Chile Undercurrent. *Geophysical Research Letters*, Vol. 29(12), pp.28-31.

Reynolds R. W. (1998) [accessed June 2012]: www.esrl.noaa.gov.

Risien C. M. & Chelton D. B., 2008. A Global Climatology of Surface Wind and Wind Stress Fields from Eight Years of QuikSCAT Scatterometer Data. *American Meteorological Society*, pp.2379-2413.

Rouault, M. et al., 2007. Propagating and origin of warm anomalies in the Angola Benguela upwelling system in 2001. *Journal of Marine Systems*, Vol. 68, pp. 473-488.

Rouault, M., 2012. Bi-annual intrusion of tropical water in the northern Benguela upwelling. *Geophysical Research Letters*, Vol. 39(May), pp.2-7.

Shannon, L. V., et al., 1986. On the existence of an El Niño-type phenomenon in the Benguela System. *Journal of Marine Research*, 44, pp.495-520.

Shannon L. V., et al., 1987. Large- and mesoscale features of the Angola- Benguela front. *South African Journal of Marine Science*, Vol. 5, pp.37-41.

Shillington, F.A. et al., 2006. Large Scale Physical Variability of the Benguela Current Large Marine Ecosystem (BCLME). *Large Marine Ecosystems*, Vol. 14, pp.15-30.

Skogen, M.D., 2010. A biophysical model applied to the Benguela upwelling system. *South African Journal of Marine Science*, (March 2012), pp.37-41.

Smith R.L., 1989. An introduction & historical review. Coastal & Estuarine Studies: Poleward Flows Along Eastern Ocean Boundaries, *Springer-Verlag.* Vol. 34, pp. 2-17.

Suginohara, N., 1982. Coastal Upwelling: Onshore-Offshore Circulation, Equatorward Coastal Jet and Poleward Undercurrent over a Continental Shelf-Slope. *Journal of Physical Oceanography*, 12, pp.272-284.

Timmermann, R., et al., 2005. On the representation of high latitude processes in the ORCA-LIM global coupled sea ice – ocean model. *Ocean Modelling*, 8, pp.175-201.

Veitch, J. a., Florenchie, P. & Shillington, F. a., 2006. Seasonal and interannual fluctuations of the Angola–Benguela Frontal Zone (ABFZ) using 4.5 km resolution satellite imagery from 1982 to 1999. *International Journal of Remote Sensing*, 27(5), pp.987-998.

Veitch, J., Penven, P. & Shillington, F., 2009. Progress in Oceanography The Benguela : A laboratory for comparative modeling studies.

Veitch, J., Penven,P., Shillington, F., 2010. Modeling Equilibrium Dynamics of the Benguela Current System. *Journal of Physical Oceanography*, 40, pp.1942-1964.

von Bodungen, B. et al., 2008. Hydrographic and biological patterns across the Angola–Benguela Frontal Zone under undisturbed conditions. *Journal of Marine Systems*, 74(1-2), pp.189-215.

Appendix A

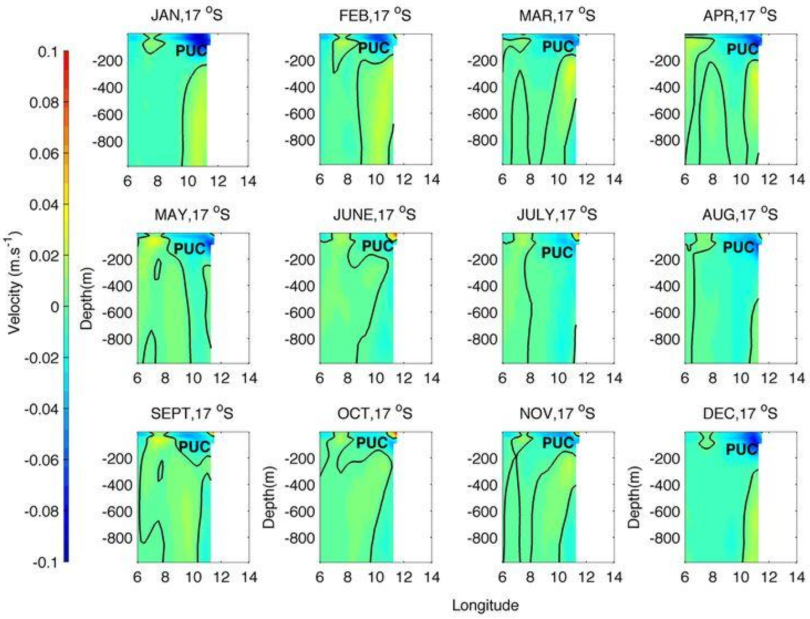

Figure 1: representation of monthly climatologies at 17 °S of mean velocities. PUC = poleward undercurrent.

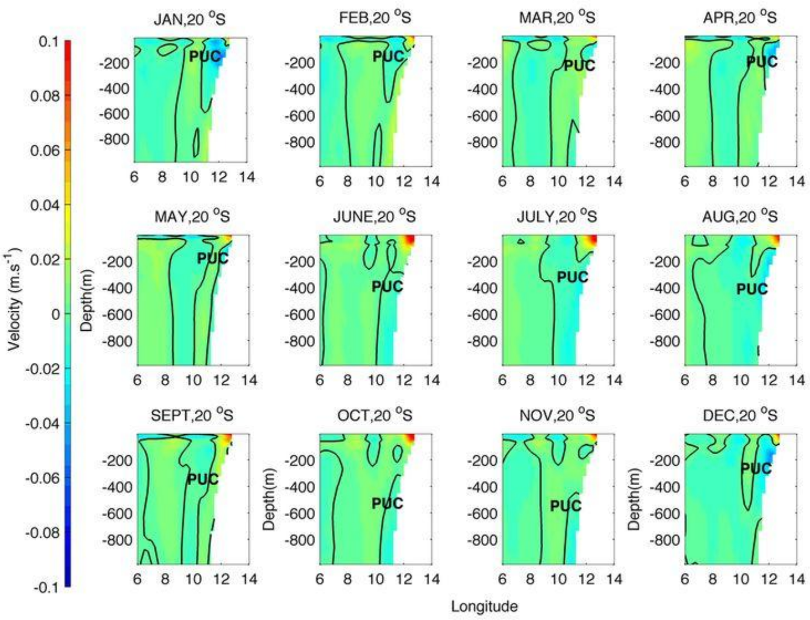

Figure 2: representation of the monthly climatologies at 20 °S of mean velocities. PUC= poleward undercurrent.

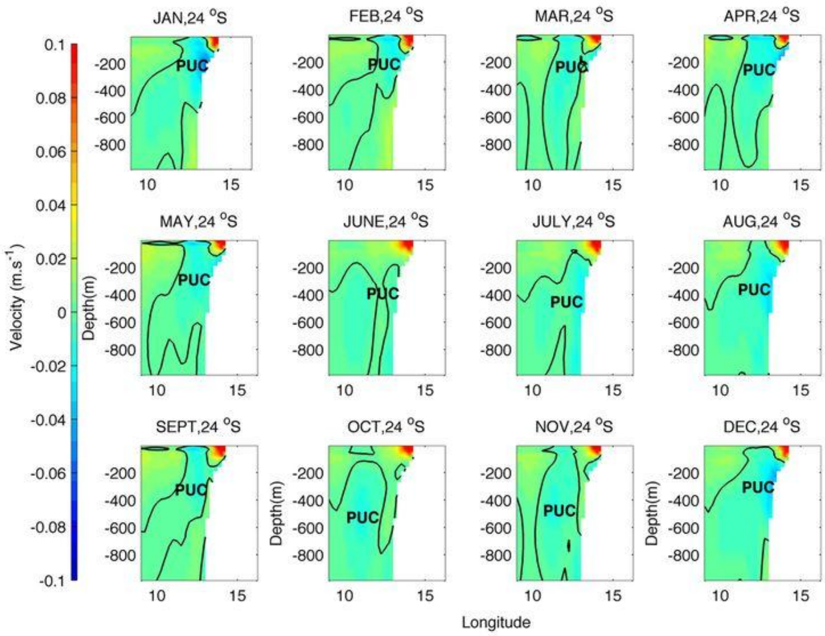

Figure 3: representation of monthly climatologies at 24 °S of mean velocities. PUC= poleward undercurrent.

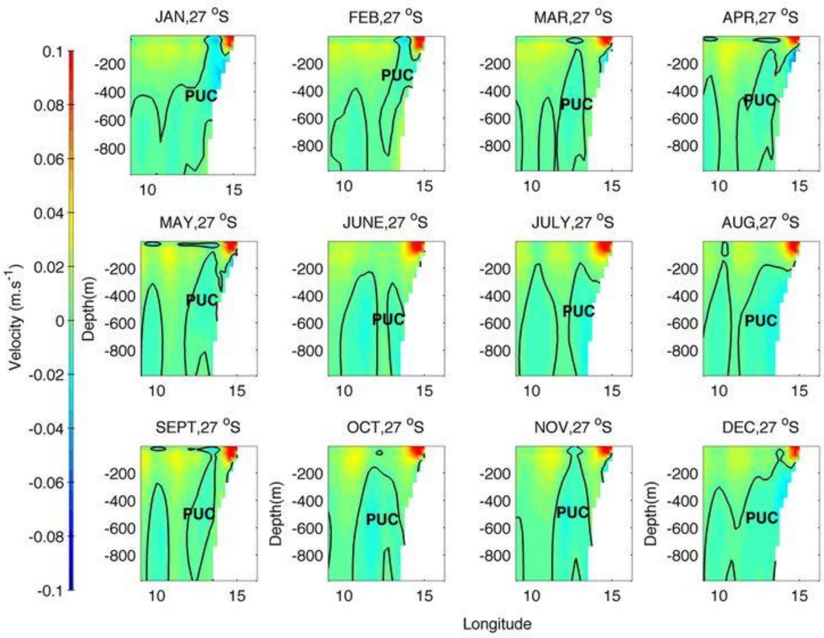

Figure 4: representation of monthly climatologies at 27 °S of mean velocities. PUC= poleward undercurrent.

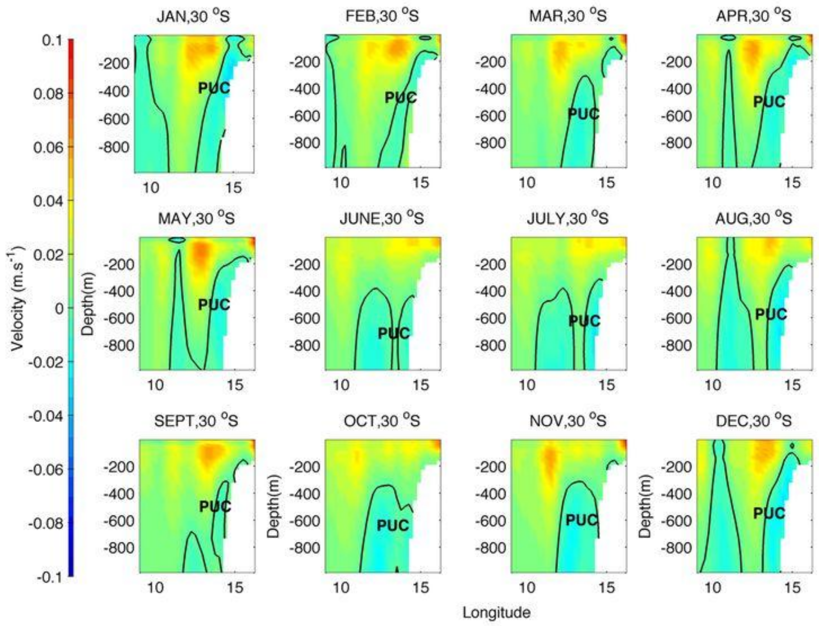

Figure 5: representation of monthly climatologies at 30 °S of mean velocities. PUC= poleward undercurrent.

Appendix B

The vorticity equation

Sverdrup relation

The derive the Sverdrup relation it was started with the momentum equations, where the Rossby number and the horizontal Ekman numbers are small, so that the advection terms can be neglected:

$$0 = fv - \frac{1}{\rho_0}\frac{\partial P}{\partial x} + \frac{\partial}{\partial z}\left(A_v \frac{\partial u}{\partial z}\right)$$

(B1)

$$0 = -fu - \frac{1}{\rho_0}\frac{\partial P}{\partial y} + \frac{\partial}{\partial z}\left(A_v \frac{\partial v}{\partial z}\right)$$

(B2)

The curl of equations B1 and B2 (i.e. $-\frac{d}{dy}$ of equation B1 $+\frac{d}{dx}$ of equation B2) is used and the continuity equation $\left(\frac{\partial u}{\partial x} + \frac{\partial v}{\partial y} = -\frac{\partial w}{\partial z}\right)$ is used to simplify the solution

$$0 = f\frac{\partial w}{\partial z} - v\beta + curl_z\left[\frac{\partial}{\partial z}\left(A_v \frac{\partial u}{\partial z}\right), \frac{\partial}{\partial z}\left(A_v \frac{\partial v}{\partial z}\right)\right]$$

(B3)

where, $f\frac{\partial w}{\partial z}$ is the vortex stretching term, β is the meridional change of the Coriolis effect , $\frac{\partial f}{\partial y}$.

B3 can be integrated with depth to a level of no motion; however, here a depth to 1000 m was used. A rigid lid assumption was made, so that $\frac{\partial w}{\partial z} = 0$ and the vortex stretching term can be neglected.

Thus left with the Sverdrup relation:

(B4)
$$0 = -\beta \int_{-1000}^{0} v dz + \frac{1}{\rho_0} \left(\frac{\partial \tau_x^s}{\partial y} - \frac{\partial \tau_y^s}{\partial x} \right)$$

where, $A_v \frac{\partial u}{\partial z} = \frac{\tau_x^s}{\rho_o}$ and $A_v \frac{\partial u}{\partial z} = \frac{\tau_y^s}{\rho_o}$.

The equation B4 can be written as:

(B5)
$$-\beta \frac{\partial \psi}{\partial x} = \frac{1}{\rho_0} \nabla \times \tau^s$$

where, ψ is the transport stream function $M_y = -\frac{\partial \psi}{\partial x}$ and $M_y = \int_{-1000}^{0} v dz$.

Or can be written as:

(B6)
$$\beta V = \frac{\nabla \times \tau_s}{\rho_0}$$

where $V = \int_{-1000}^{0} v dz.$